



HAL
open science

Shoreface mesoscale morphodynamics: A review

Klervi Hamon-Kerivel, Andrew Cooper, Derek Jackson, Mouncef Sedrati,
Emilia Guisado Pintado

► **To cite this version:**

Klervi Hamon-Kerivel, Andrew Cooper, Derek Jackson, Mouncef Sedrati, Emilia Guisado Pintado. Shoreface mesoscale morphodynamics: A review. *Earth-Science Reviews*, 2020, 209, pp.103330. 10.1016/j.earscirev.2020.103330 . hal-02944352

HAL Id: hal-02944352

<https://hal.science/hal-02944352v1>

Submitted on 8 Oct 2021

HAL is a multi-disciplinary open access archive for the deposit and dissemination of scientific research documents, whether they are published or not. The documents may come from teaching and research institutions in France or abroad, or from public or private research centers.

L'archive ouverte pluridisciplinaire **HAL**, est destinée au dépôt et à la diffusion de documents scientifiques de niveau recherche, publiés ou non, émanant des établissements d'enseignement et de recherche français ou étrangers, des laboratoires publics ou privés.

1 **Shoreface mesoscale morphodynamics: a review**

2 Klervi Hamon-Kerivel (1) *, Andrew Cooper (1,2), Derek Jackson (1,2), Mouncef Sedrati (3), Emilia
3 Guisado Pintado (4,1)

4 (1) School of Geography & Environmental Sciences, Ulster University, Coleraine, UK,

5 (2) Discipline of Geology, University of KwaZulu-Natal, Westville Campus, Private Bag X54001, Durban
6 4000, South Africa

7 (3) Équipe GMGL-Domains Océaniques UMR 6538, Université de Bretagne Sud, Vannes, France,

8 (4) Geography Regional Analysis and Physical Geography, University of Seville, Seville, Spain

9

10 *Corresponding author: School of Geography & Environmental Sciences, Ulster University, Cromore
11 Road, Coleraine BT52 1SA, UK; Email Address: Hamon_Kerivel-k@ulster.ac.uk

12 **Abstract**

13 At seasonal to century timescales (mesoscale), the shoreface is a critical zone seaward of the surf zone
14 and/or beachface, in which waves interact with the mobile seafloor to cause morphological change.
15 This has important (and often unacknowledged) implications for adjacent shoreline form and
16 behaviour both now and in the near-future. The shoreface has been relatively little studied from a
17 mesoscale morphodynamic (morphological change over time) perspective and various definitions
18 exist regarding its extent and morphodynamic subdivisions. To overcome the diversity and ambiguity
19 of existing definitions we propose a standard terminology involving the external limits and
20 subordinate zones of the shoreface.

21 In our definition, the landward limit of the shoreface coincides with the seaward limit of the fair
22 weather surf zone, and where no surf zone is present, the base of the beachface. The shoreface itself
23 is subdivided into upper and lower shorefaces, separated by the depth of closure (DoC) as defined by
24 Hallermeier (1981). The seaward limit of the lower shoreface is defined by the limit of significant
25 sediment transport, indicated by bed shear stress according to Valiente et al. (2019). All boundaries
26 are temporally variable according to wave characteristics and timescale of study.

27 The upper shoreface is dynamic at seasonal to annual timescales and interacts with the adjacent
28 surfzone via wave transformation and two-way sediment exchange. The lower shoreface is dynamic
29 at decadal to millennial timescales and it interacts with the adjacent upper shoreface and inner shelf.
30 The upper shoreface is strongly influenced by wave hydrodynamics whereas the lower shoreface is
31 less dynamic and its shape is more heavily influenced by geological factors (nature and/or abundance
32 of sediment, depth and erodibility of rock outcrop, etc.). Sediment exchange both within the shoreface
33 and between shoreface and adjacent environments is strongly event-driven. Longshore, onshore and
34 offshore transport mechanisms have been documented.

35 The shoreface profile influences, and is influenced by, wave transformation, however, the widely
36 adopted shoreface equilibrium profile is not universally applicable. Instead, a diversity of shoreface
37 morphologies exists in two and three dimensions. These are likely related to sediment supply and
38 accommodation and we propose a spectrum of shoreface types based on these variables. Recent
39 studies have shown that large-scale 3-D forms (e.g. shoreface-connected ridges and sorted bedforms)
40 strongly influence shoreline behaviour, however, the dynamics of these shoreface bedforms requires
41 further investigation. Each type of shoreface likely exhibits distinctive behaviour at the mesoscale
42 (time scale of 10^1 to 10^2 years and a spatial scale of 10^1 to 10^2 km). This is proposed as a unifying model
43 with which to integrate studies of shoreface dynamics at different spatial and temporal scales.

44 **Keywords**

45 Shoreface morphodynamics

46 Depth of closure

47 Mesoscale

48 Shoreline

49 Shoreface Connected Ridges

50

51 **1. Introduction**

52 The shoreface is a transitional zone between the continental shelf and the shoreline, in which waves
53 (particularly long period waves) begin to strongly interact with the seabed. These shoreface
54 interactions “condition” the waves, altering their deep water parameters, before they reach the surf
55 zone where more significant wave-seabed interactions (attenuation, breaking and generation of
56 secondary wave motions) occur (Wright and Short, 1984). The contemporary shoreface is difficult to
57 access and direct measurements have been eclipsed until recently by a strong scientific and
58 engineering focus on the surf zone and beach face (swash zone) and areas to landward. Geologically,
59 the shoreface comprises a series of sandy deposits which reflect the influence of waves, currents and
60 organisms on the palaeo-environment (Dashtgard et al., 2009; Hampson and Storms, 2003).

61 The influence of the shoreface on incoming wave transformation, particularly during storms, is widely
62 recognised (Backstrom et al., 2015; Héquette and Hill, 1993; Niedoroda et al., 1984; Swift et al., 1985)
63 and has been the subject of research attention in recent years (Backstrom et al., 2015). Interest has
64 also been stimulated by recognition of the shoreface’s role in coastal response to sea-level rise
65 (Cooper et al., 2018) and its role as a reservoir of sediment accumulated during and since the Holocene
66 transgression (Kinsela et al., 2016). Ancient shoreface sediments have also been studied because they
67 can form hydrocarbon reservoirs (Howell et al., 2008). This paper reviews past research and recent
68 progress in understanding the shoreface in the context of the wider coastal system. It reviews linkages
69 between the shoreface and adjacent surf zone and shoreline and explores the variety of shoreface
70 morphologies and the influences upon it such as geological control and sediment availability.

71 This paper is largely concerned with shoreface morphology and mesoscale (dynamics which
72 corresponds to a time scale of 10^1 to 10^2 years; and a spatial scale of 10^1 to 10^2 km) which is the typical
73 spatiotemporal scale of morphological change. From a review of existing literature we propose a
74 consistent definition and present a new classification according to shoreface morphologies,. The lack
75 of a uniform definition of “shoreface”, and its variation in meaning for different disciplines (coastal

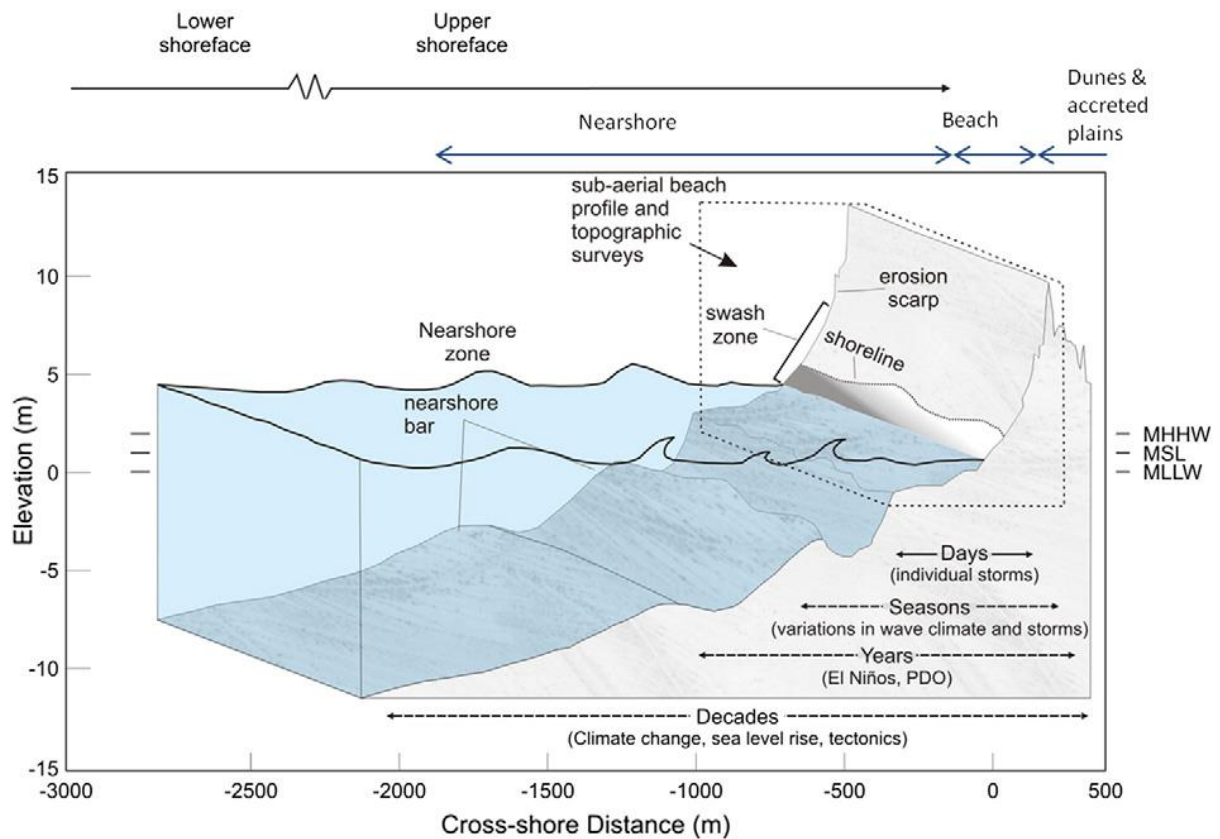
76 engineering, geology, oceanography...) has led to discrepancies in terminology. While this is addressed
77 in the next section of the review , from this point on we refer to the shoreface as the transitional zone
78 between shelf and beach, delimited on the shoreward limited shore side by the (fairweather) surf
79 zone (or swash zone) and seaward by the threshold beyond which sediment transport is no longer
80 intense enough to contribute to the overall coastal dynamics at a mesoscale (time scale of 10^1 to 10^2
81 years and a spatial scale of 10^1 to 10^2 km). However the shoreface exhibits changes at other spatio-
82 temporal scale, this will be explicated below.

83

84

85 **2. Definition of the shoreface**

86 The shoreface can be loosely defined as the transition zone between the beach and the shelf (**Figure**
87 **1**). Definitions of its shoreward and seaward limits and internal subdivision are still not fully agreed
88 upon. Some authors (Ortiz and Ashton, 2016; Thielert et al., 2001, 1995) suggest the subaerial coastal
89 zone itself represents the shoreward boundary, thus including the surf zone (Niedoroda et al., 1984)
90 or the lower limit of the swash (Aagaard et al., 2013). Others (Backstrom et al., 2007; Héquette and
91 Hill, 1993; Héquette et al., 2001; Wright et al., 1991, 1991) place the landward boundary between the
92 shoreface and the surf zone. Green et al. (2004) refer specifically to the 'breakpoint' as the landward
93 limit of the shoreface. On beaches without surf zones e.g. Caribbean beaches (Boon and Green, 1988),
94 the shoreface might extend landward to the beach step and swash zone.



95

96 **Figure 1.** (colour) Conceptual diagram of the current definition and limits of the shoreface (from Ruggiero et al. (2016))

97 The seaward limit is equally contentious due largely to the fact that it is often hard to identify a
 98 definitive morphological feature (e.g. a break in slope) or change in texture between the shoreface
 99 and the continental shelf. Without a physical reference location the spatially and temporally variable
 100 point at which waves start to mobilise sediment (i.e. in other words the wave base where waves begin
 101 to interact with the sea bed sediment) is normally used (Aagaard, 2014; Dashtgard et al., 2012; Stive
 102 and De Vriend, 1995). Wave base is temporally variable and hence a definition of the timescale for
 103 assessment of wave base is required (see section 4.).

104 The shoreface can also be defined in terms of the physical processes that occur within it. Héquette et
 105 al. (2008a, p. 227) proposed that the shoreface is 'the shallow, friction-dominated zone where the
 106 response of the seabed to hydro-meteorological forcing results from the complex interactions
 107 between wind, waves and currents'. In this process-based approach, the shoreface comprises two
 108 sections: the *upper shoreface* which is influenced by wave-breaking processes and the dissipation of

109 wave energy (i.e. the surf zone in other definitions) and the *lower shoreface* that is dominated by wave
110 shoaling (Aagaard, 2014; Stive and De Vriend, 1995). The shoreface is a wave-affected zone (Swift et
111 al., 1985; Wright et al., 1991), even at its seaward, deepest point. Incoming waves impact the bottom
112 from a starting point commonly defined as the wave base until they reach the shore. This definition is
113 similar to the profile zonation proposed by Hallermeier (1981) that introduced potentially calculable
114 depths for the boundaries between upper and lower shoreface and between lower shoreface and
115 shelf (Cowell et al., 1999) based on wave parameters. In this definition, the upper shoreface is the
116 zone most likely to experience strong seasonal variability and is therefore equivalent to the shoreface
117 ‘active zone’ as defined by Stive and De Vriend (1995), with its seaward boundary being the depth of
118 closure as calculated using Hallermeier (1978) formula. In this zonation, the lower shoreface is
119 bounded seaward by the calculated maximum water depth for initiation of motion (wave base) under
120 annual median wave conditions. However, the depth of closure and maximum depth for wave-
121 initiated motion are temporally variable parameters and cannot be considered an absolute calculable
122 boundary for the shoreface.

123 Other authors have proposed discriminating the shoreface according to slope (Swift et al., 1985) or
124 sediment type and characteristics (Aragonés et al., 2018; Cowell et al., 1999; George and Hill, 2008).
125 Larson et al. (1999) examined the theoretical profile under breaking (surf zone, upper shoreface) and
126 non-breaking (shoaling wave condition, lower shoreface) and determined that the ‘equilibrium profile’
127 (see section 3) of the lower shoreface is for that instance distinguished from the upper shoreface by a
128 lower curvature than the one of the upper shoreface. Indeed, the separation between upper and
129 lower shoreface zones is sometime set at a discernible break in slope (Niedoroda et al., 1984).

130 In general use, the term ‘shoreface’, when not more fully specified, appears to refer to the lower
131 shoreface, as most authors equate it with an environment dominated by wave shoaling that is active
132 only at a long time scale, i.e decades and longer (Aagaard, 2014; Green et al., 2004; Héquette et al.,
133 2008a; Niedoroda et al., 1984). In current usage, the ‘upper shoreface’ therefore corresponds to a

134 seasonally active zone that sometimes, but not always, includes the surf zone. Typically, the upper
135 shoreface is the zone influenced by the offshore migration of the surf zone during storm conditions
136 that results in morphological changes at a seasonal time scale. This inconsistency in terminology
137 regarding the shoreface can be confusing. Subsequently, we propose a standard definition.

138

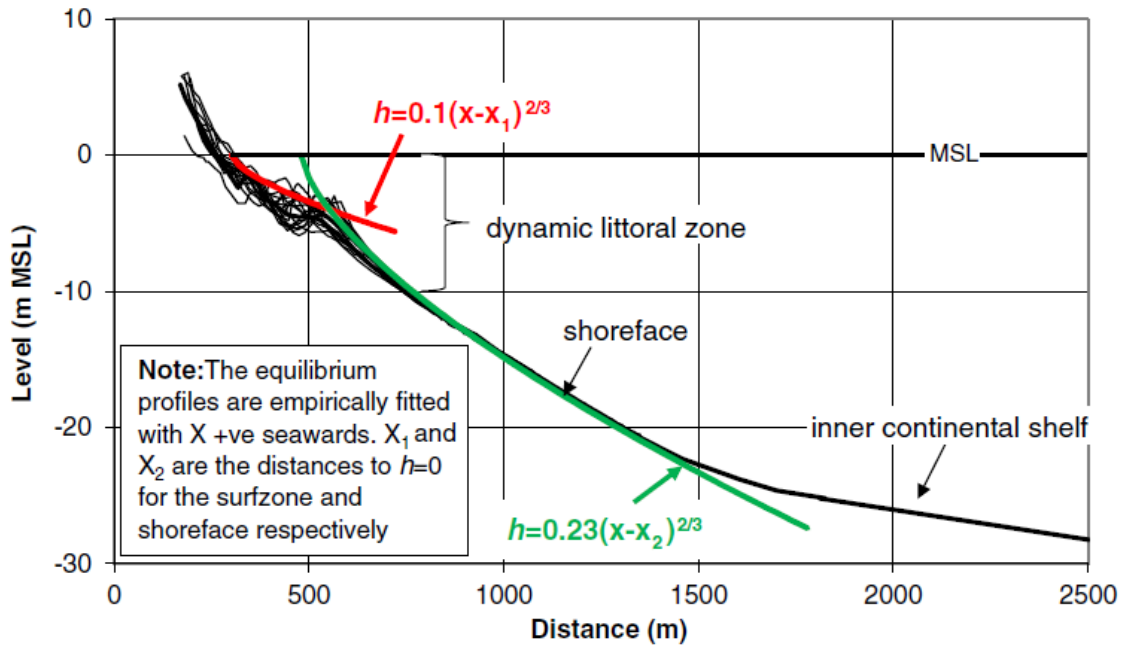
139 **3. Shoreface equilibrium profile**

140 Most models of beach/shoreface profiles are based on the assumption of the existence of an
141 equilibrium profile. The equilibrium profile in the literature has its origins as far back as Fenneman
142 (1902, p. 1) who wrote: “There is a profile of equilibrium which the water would ultimately impart, if
143 allowed to carry its work to completion”. This concept is still widespread in coastal evolution models,
144 especially in engineering applications (Cooper and Pilkey, 2004).

145 The profile of equilibrium can be defined as the theoretical, two-dimensional shape achieved by a
146 sand-rich, unconstrained coastal system under a given stable wave climate and sediment type. These
147 are the conditions of flume tank experiments that were first used to explore the concept of equilibrium
148 profile (Dean, 1991). In theory, when the system is in equilibrium then no net sand transport occurs
149 and the rate of dissipation is constant. It is the result of an equilibrium between onshore directed
150 (constructive) sediment transport and offshore (destructive) sediment flow and is usually concave
151 upward as described by Dean (1991). Its form is described by an empirical equation of the form:

$$157 \quad h(y) = Ay^n$$

152 where: $h(y)$ is the water depth h at distance offshore y , A is a scale parameter (dependent on grain
153 size) and ‘ n ’ is a parameter commonly set at $2/3$ (the best fit to field data found by (Dean, 1977))
154 (**Figure 2**). The profile of equilibrium of a coastal system can also be obtained from field data by
155 analysing a time series of cross-shore profiles (Birkemeier, 1985; Hinton and Nicholls, 1999; Nicholls
156 et al., 1998; Różyński et al., 1999).



158

159 *Figure 2.(colour) Example of equilibrium profiles fitted for the surf zone and shoreface on the Australian Gold Coast (from:*
 160 *Patterson and Nielsen 2016). In this example, the dynamic littoral zone equates to the surf zone and upper shoreface.*

161 Pilkey et al. (1993) reviewed the principle of equilibrium profile and demonstrated that the conditions
 162 (i.e. a sand-rich system not affected by transient sand bodies or underlying geology and closed by an
 163 offshore boundary) that are required for an equilibrium are unrealistic assumptions in a natural
 164 environment. Pilkey et al. (1993) also pointed out that the equilibrium equation is flawed because the
 165 only variable influencing the shape of the profile is the grain size (expressed as A) and the wave climate
 166 and inherited morphology have no influence. Similarly, Thieler et al. (1995), pointed out the
 167 inconsistent grain size across the shoreface which cannot be accounted for by a single number (A in
 168 Dean's equation). They also showed that the apparent relationship between ' A ' and grain size is not
 169 evident when only sand grain sizes are considered. Those authors also demonstrated the major control
 170 played by underlying geology on shoreface morphology.

171 Backstrom et al. (2007) showed from field measurements that adjacent shorefaces could have
 172 markedly different shapes that diverged from potential 'equilibrium' profiles. While one of the sites
 173 displayed a concave-up type morphology closer to 'typical equilibrium profile' the other had a linear
 174 to convex profile. The presence of other convex morphologies on shorefaces worldwide (Aleman et

175 al., 2015; Green et al., 2004; McNinch, 2004; Miselis and McNinch, 2006) rules out the concave upward
176 equilibrium profile morphology as a universal principle, as do shorefaces whose morphologies are
177 influenced by rock outcrop and sub-crop (Browder and McNinch, 2006; Riggs et al., 1995; Thieler et
178 al., 1995).

179 While the principle of equilibrium is a valid concept to describe the evolution of an idealized coastal
180 system, it appears to have limited applicability for “real-world” situations (Athanasidou et al., 2019;
181 Pilkey et al., 1993; Thieler et al., 1995). This is mostly because the forces that affect morphology and
182 drive morphological change on the shoreface appear to be controlled, at least in part, by factors other
183 than waves and grain size. Clifton (2005), states that for a transgressive shoreface profile (which make
184 up the majority of the world’s coasts (Bird, 1985)) only the upper part is “wave-tuned” and
185 theoretically able to attain equilibrium, while the lower part of the profile is shaped by differential
186 erosion due to the presence of older deposits.

187 Extensive research has been conducted on the “active” part of the profile and its influence on
188 shoreline and beach dynamics. This is particularly pertinent when considering seasonal variation,
189 event scale (storm) dynamics and shoreline variability. Most coastal evolution models also focus on
190 this zone because the lower part of the shoreface lies beyond the “depth of closure” and its dynamics
191 are considered to only be significant during storm events when sand is ‘lost’ (i.e. transported from the
192 upper shoreface to the lower shoreface) (Cowell et al., 1995; Stive and De Vriend, 1995).

193 While the shoreface has mostly been considered two-dimensionally, it has become more evident that
194 longshore variations often exist and that many shorefaces are strongly three-dimensional. This is
195 related to the presence of various sedimentary features (see section 7) and/or the influence of the
196 geological framework (see section 6).

197

198 **4. Depth of closure and the shoreface**

199 The depth of closure commonly refers to the seaward limit at which morphological change is not
200 observable for a (usually seasonal) period of time; it also commonly is regarded as the boundary
201 between upper and lower shoreface (Cowell et al., 1999)

202 The depth of closure can be determined by analysing a time series of profiles at a given location
203 (Różyński et al., 1999) or consecutive bathymetry datasets (Robertson et al., 2007) to identify the
204 depth at which the change in morphology becomes insignificant (not measurable), keeping in mind
205 that the depth of closure is related to the time-scale of the measurements and to the measurement
206 accuracy (Hoekstra et al., 1999). Various statistical methods also exist to identify this threshold (Kraus
207 and Harikaj, 1983; Nicholls et al., 1997). However, most commonly, and because datasets necessary
208 to determine the depth of closure are relatively rare, the DoC is usually calculated from wave
209 parameters.

210 Depth of closure calculations were introduced by Hallermeier (1981, 1978). Hallermeier's DoC
211 calculation is based on the wave period and height and determines the closure depth (dI) for an annual
212 wave return period.

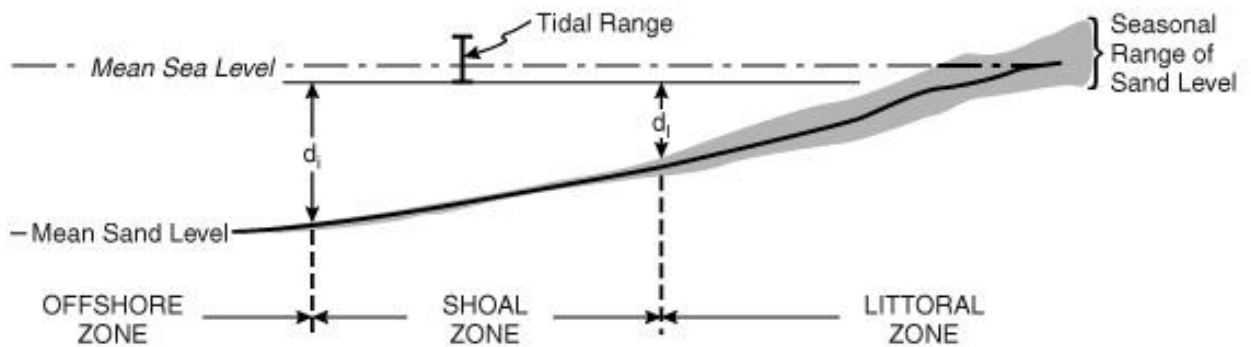
$$213 \quad dI = 2.28Hs - 68.5 \left(\frac{Hs^2}{gTs^2} \right)$$

214 With Hs the local significant wave height and Ts the significant wave period.

215 Related to depth of closure is the wave base, referred to by Hallermeier (1981) as the outer depth of
216 closure (di) (as opposed to the DoC which is referred to as the inner depth of closure (dI)) (**Figure 3**).
217 The outer DoC was defined as "maximum depth for motion initiation by median wave conditions" by
218 (Hallermeier, 1981) and corresponds to the limit of wave-initiated cross-shore sediment transport, or
219 the seaward limit of the wave-constructed profile. It is defined as the depth at which the incident wave
220 reaching the shore begins to shoal and can be calculated using:

$$221 \quad di = (Hs - 0.3 \sigma) Ts \left(\frac{g}{5000D} \right)^{0.5}$$

222 With H_s the mean significant wave height, σ the standard deviation of significant height, T_s the mean
 223 significant period, g the acceleration of gravity and D the sand diameter.



224

225 **Figure 3.** Definition of inner and outer depth of closure (Hallermeier, 1981) with d_i the inner depth of closure (DoC) and d_o the
 226 outer depth of closure or wave base. Here, the littoral zone corresponds to the upper shoreface and the lower shoreface is
 227 included in the shoal zone.

228 Subsequent studies (Nicholls et al., 1997) building on the work of Hallermeier (1981, 1978) have shown
 229 that the depth at which closure is calculated is highly time-variable, and it increases with the time-
 230 scale involved (Nicholls et al., 1999, 1998). It is therefore customary to associate a depth of closure
 231 with a temporal dimension. The DoC can be calculated for a specific event (Robertson et al., 2008),
 232 but more commonly it is calculated for yearly/ seasonal variations or even over a number of years
 233 (Valiente et al., 2019) up to decades (Hinton and Nicholls, 1999) and even millennia (Ortiz and Ashton,
 234 2016). Similarly, the wave base depth is usually calculated for a typical year. And as with the DoC, it
 235 varies with the return period used for the calculation

236 The depth of closure is also known to be variable in the longshore (Hinton and Nicholls, 1999; Sabatier
 237 et al., 2005) with influences exerted by sedimentology and underlying geology (Robertson et al., 2008),
 238 as well as wave exposure.

239 While most of the literature has focused on the depth of closure, recent studies have proposed new
 240 calculations for the lower shoreface/ shelf threshold and advanced the definition of the seaward limit
 241 of the shoreface. For example. Ortiz and Ashton (2016) introduced the notion of morphodynamic

242 depth of closure (MDOC) defined as the depth beyond which 'evolution of the shoreface becomes
243 geologically slow and the bed shape response to environmental change becomes virtually non-
244 existent'. Ortiz and Aston's (2016) calculated MDOC is dependent on wave height and period but is
245 not affected by the sediment grain size; it only influences the shape of the modelled equilibrium
246 profile. This method of calculation, which proposes a calculation of the depth at which morphological
247 variability is geologically slow (millennia), is relevant to studies of shoreface morphodynamics and
248 more generally to the study of macro-scale (time scale $>10^1$ years and spatial scale $>10^2$ km) coastal
249 behaviour.

250 Valiente et al. (2019) used wave bed shear stress to estimate the seaward limit of significant sediment
251 transport (contributing to the overall coastal dynamics). This depth of transport (DoT) outer limit takes
252 into account both wave-induced stress and stress induced by tidal currents. Their approach makes the
253 distinction between DoC which limits the zone of significant morphological change i.e. the upper
254 shoreface (which can be approximated by Hallermeier's formulation) and the DoT that delimits the
255 zone of significant sediment transport. The use of bed shear stress permits identification of the zone
256 where sediment transport is significant in terms of volume but where no morphological changes are
257 observable at the medium term (10^0 to 10^1 years). It is therefore a good potential proxy for the lower
258 shoreface/shelf boundary, as it determines the extent of the active shoreface. In contrast, the wave
259 base (DoC) only encompasses the wave-affected areas of the shelf where significant morphological
260 change is observed.

261 For the upper/ lower shoreface limit, several methods of DoC identification exist. For example,
262 Aragonés et al. (2018) proposed that DoC could be defined as 'the point where the minimum size of
263 sediment is located'. Aragonés et al. (2019) further proposed a numerical model based on wave
264 parameters and sedimentology to determine the depth of closure.

265 In the absence of actual measurements, calculated depth of closure is still widely used to characterise
266 coastal systems, especially for engineering purposes. This approach, however, is not universally

267 applicable especially where rock outcrops or limited sand supply constrain sediment transport on the
268 shoreface. Miselis and McNinch (2006), for example, showed that using calculated depth of closure
269 can cause an over-estimation of the volume of nearshore sediment in geologically (vertically)
270 constrained areas.

271

272 **5. Shoreface hydrodynamics**

273 Waves have an oscillatory motion that is modified by the interaction with seabed as they cross the
274 shoreface. Incoming waves dissipate energy over the shoreface and this may lead to sediment
275 transport and morphological evolution (Roelvink and Stive, 1991). When the critical bottom friction is
276 reached, seabed sediment starts to be transported either as suspension or as bed load, making
277 incoming waves one of the main driving factors for sediment transport in the coastal zone. Over the
278 shoreface, because of diminishing depths, waves shoal before breaking in the surf zone. Shoaling
279 creates an asymmetry in the wave oscillation, resulting in net sediment transport directed toward the
280 shore (Austin et al., 2009; Huisman et al., 2019; Niedoroda and Swift, 1981). This is especially true
281 under fair-weather conditions when wave oscillation asymmetry is the main process driving onshore
282 sediment transport (Niedoroda and Swift, 1981; Niedoroda et al., 1984; Swift et al., 1985). Incoming
283 waves can also create steady currents such as undertow and rip currents, particularly in the surf zone.
284 These are strongly related to morphology and beach slope (Castelle et al., 2016). These flows are
285 directed offshore and tend to transport sediment from the surf zone to the shoreface, particularly
286 during high-energy storm conditions (Loureiro et al., 2012a). The importance of infragravity waves on
287 cross-shore sediment transport is still unclear (Bakker et al., 2016; Bertin et al., 2018) but it has been
288 hypothesised that they can contribute to offshore transport during storms (Russell, 1993).

289 Another factor influencing sediment transport in the coastal zone is wind. Currents generated by
290 winds can be drivers of sediment transport, especially down-welling currents that, during storms, have
291 the capacity to move sediment offshore (Héquette and Hill, 1993; Héquette et al., 2001; Niedoroda et

292 al., 1984). Swift et al. (1985) pointed out the importance of wind-driven coastal flow for the sediment
293 budget, especially when intensified by storms, stating (p. 332) that “Because of the offshore
294 component of bottom flow, sand is swept down the lower shoreface and onto the adjacent shelf. Fair
295 weather processes may be unable to return storm-deposited sand to the beach from such an offshore
296 position”.

297 Wind forcing may also affect the tidal current velocity by reinforcing or limiting it depending on the
298 concordance of wind and current direction (Héquette et al., 2008a). It also causes near-bottom
299 currents which affect sand ridge migration (Guerrero et al., 2018) (see below in section 7).

300 Tidal currents can also be a significant component in sediment transport on shorefaces. On microtidal
301 shorefaces, tidal currents are generally overlooked. Moreover, since tidal currents are often
302 symmetrical their significance can be limited when averaged over a tidal cycle (Niedoroda et al., 1984).
303 On shorefaces where morphology creates tidal asymmetry, however, sediment transport from
304 residual tidal currents is non-negligible whereas, in meso- and macrotidal environments, tidal currents
305 are fundamental in driving sediment transport (King et al., 2019; Valiente et al., 2019). In their study
306 of sediment transport on a tide dominated (macrotidal) shoreface environment, Héquette et al.
307 (2008a) found that, although waves were the main forcing parameter in mobilising sediment as they
308 cross the shoreface, sediment transport vectors were linked to average currents directed alongshore,
309 in particular, tidal currents.

310 Hydrodynamics on the shoreface potentially involve a combination of wave, wind and tidal current
311 action. These processes can interact via positive or negative feedback. For example, winds can play a
312 role in enhancing or inhibiting tidal currents depending on the relative direction of both those forces
313 (Héquette et al., 2008b). During storm wave events, the combined action of waves and winds tends
314 to create offshore-directed currents that move sediment to the lower parts of the shoreface and shelf
315 (Héquette et al., 2001; Niedoroda and Swift, 1981; Wright et al., 1991) whereas, under fair weather
316 conditions, smaller waves tend to move sediment onshore (Wright et al., 1991). As most mean

317 currents (i.e. rip currents, undertow, down-welling) are directed seaward, onshore sediment transport
318 only occurs under favourable conditions for a limited time. Wright et al. (1991, p. 46) found that at
319 Duck beach (North Carolina, USA), storms were “capable of transporting more sand offshore in an
320 hour than fairweather processes can move onshore in two or more days”.

321 Over longer time scales (10^0 to 10^1 years), the variability in shoreface morphology may be influenced
322 by climatic factors such as ocean circulation patterns or oscillation. In particular, El Niño/ La Niña
323 periods have been shown to have specific impacts (shift in sediment transport and morphological
324 responses) on the coast and shoreface (Goodwin et al., 2013; Ruggiero et al., 2005; Wright et al.,
325 1991). Other factors such as storm grouping (Lee et al., 1998; Loureiro et al., 2012b) also exert a
326 control on shoreface dynamics. Indeed, a series of storms often has a more extreme effect than a
327 single (even more energetic) storm in creating morphological changes and causing erosion of the
328 beach and upper shoreface and transport of sediment to the lower shoreface (Guisado-Pintado and
329 Jackson, 2019, 2018).

330

331 **6. Geological influences on the shoreface**

332 It has been shown that underlying geology is a limiting factor for the formation of equilibrium profiles
333 (Pilkey et al., 1993), and various studies have emphasised the role of geology and coastal morphology
334 on mesoscale coastal behaviour (Cooper et al., 2018; Gallop et al., 2020; Jackson et al., 2005). A large
335 proportion of the world’s coast is rocky and/or embayed (laterally constrained) and there is much
336 variability in sediment volume and thickness. The potential for erosion of the underlying lithology to
337 produce shoreface sediment is also highly dependent on lithology and dynamics as well as the rate of
338 sea-level rise.

339 Coasts can acquire equilibrium profiles if the shoreface is sand-rich and the underlying and offshore
340 geology does not play any part (Pilkey et al., 1993). These conditions are unrealistic for most of the

341 world's shorefaces. Typically, for the barrier island coast of North Carolina, for example, Pilkey et al.
342 (1993, p. 271) found that 'the shape of the shoreface in sediment-poor areas is determined by a
343 complex interaction between underlying geology, modern sand cover and highly variable incoming
344 wave climate'.

345 Other studies on North America's Atlantic coast confirm this observation. Riggs et al. (1995) showed
346 that the geological framework determines 3D shoreface morphology, sediment texture and
347 composition as well as shoreline recession rates, concluding (p 231) that 'each barrier beach and
348 shoreface are total products of their geologic heritage; the signature of their history controls and
349 influences the present morphology, shoreface dynamics, and rates of shoreline recession'. Thieler et
350 al. (1995) examined the variation in grain size, underlying geology and sediment transport of
351 Wrightsville Beach (North Carolina) and found a lack of homogeneity in sediment distribution and
352 irregular bathymetry that also indicated a strong control by underlying geology on sediment transport
353 processes on the shoreface.

354 The geological framework can influence both the volume of sediment available for transport but it can
355 also in some region impede sediment transport reducing the amount of sediment contributing to a
356 coastal system's sediment budget (Menier et al., 2019, 2016). Furthermore, the geological setting of
357 the shoreface and the volume of shoreface sediment readily available for transport seem to have an
358 influence on shoreline evolution pattern (see section 8.3).

359 For most coasts influenced by their geological setting, conventional theories of shoreface
360 morphodynamics are inadequate. Indeed, in geologically constrained areas it has become evident that
361 commonly accepted theory related to nearshore morphodynamics, such as equilibrium profiles (Pilkey
362 et al., 1993; Riggs et al., 1995; Thieler et al., 1995), depth of closure (Robertson et al., 2008, 2007), or
363 beach state parameters (Jackson et al., 2005; Loureiro et al., 2013) are not directly applicable.

364

365 7. Sedimentary Bedforms

366 Sedimentary bedforms on the shoreface occur at various length scales from ripples (cm) to fields of
367 multi-metric sediment-rich features known as sand ridges (km), they are the result of complex
368 hydrodynamics, including feedbacks between the seabed and tides/currents. Their formational
369 mechanisms and self-organisational processes are still unclear (Durán et al., 2018; Guerrero et al.,
370 2018; Murray et al., 2014b; Nnafie et al., 2015, 2014). In terms of shoreface dynamics, sedimentary
371 bedforms can act as possible sources/sinks of sediment and can also influence sediment
372 characteristics (sorting etc.) and nearshore hydrodynamics (via change bathymetry, bottom roughness
373 etc.) (Latapy et al., 2020; Verwaest et al., 2020).

374 The main sedimentary features present on shorefaces are sand ridges (Madricardo and Rizzetto, 2018)
375 . On macro-tidal coasts, sand ridges are mostly related to tidal hydrodynamics. They are termed tidal
376 sand ridges or tidal sand banks or waves. They originate from the hydrodynamic climate created by
377 strong tide-related currents, as stated by Anthony (2013, p. 10); “In the course of the Holocene, [...] sand
378 has been reworked by the interplay of tidal currents and storm waves into the impressive jumble
379 of tidal sand ridges and banks that have served as sources for coastal accretion.” Tidal sand banks are
380 usually sub-parallel to the shoreline and attuned to the local tidal current climate. They exist on the
381 shoreface and can migrate onshore under storm conditions at the rate of several metres per year
382 (Héquette and Aernouts, 2010; Héquette et al., 2013; Van der Molen and Van Dijck, 2000).

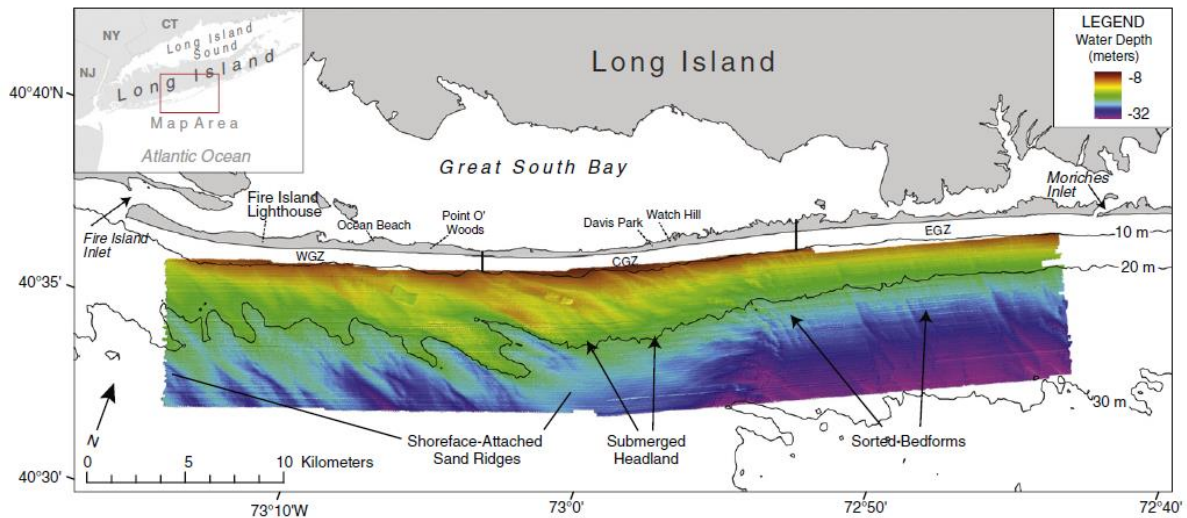
383 Sand ridges also exist on coasts where they are not the product of tidal hydrodynamics. In such cases
384 they are referred to as sand ridges, shoreface-attached sand ridges, or shoreface-connected ridges
385 (SCRs) (**Figure 4**). SCRs are shoreline-oblique, rhythmic sand ridges. The spacing between each ridge is
386 in the 1-10 km order, their height can exceed 10 m and their length more than 25 km. Found at depths
387 of 5-20 m with their landward end connected to the shoreface (hence the name), they often develop
388 at an angle of around 20° to the shoreline. They occur particularly on storm-influenced shelves and

389 can migrate with the dominant current at a rate of several meters per year (Calvete et al., 2001a,
390 2001b; Falques et al., 1999; van de Meene and van Rijn, 2000a, 2000b; Yoshikawa and Nemoto, 2014).

391 The formation processes of SCRs are rather unclear. Some suggest they are pre-Holocene
392 transgression relics (McBride and Moslow, 1991) while others have focused on the physical processes
393 necessary to create and sustain such bedforms (Calvete et al., 2001a, 2001b; Trowbridge, 1995; Vis-
394 Star et al., 2007). Their dynamics are complex (Browder and McNinch, 2006; Falques et al., 1999; Goff
395 et al., 2015; Guerrero et al., 2018; McNinch, 2004; Schupp et al., 2006) and many are assumed to have
396 formed at shallower depth and been subsequently drowned by rising sea level (Durán et al., 2018;
397 Nnafie et al., 2015, 2014).

398 Other shoreface features have been termed sorted bedforms or rippled scour depressions (RSDs)
399 (**Figure 4**). These are relatively stable features that have been widely documented. RSDs comprise
400 alternating sand and coarse gravel bands with shore-oblique to shore-normal orientation. The coarse
401 gravel is commonly rippled, while the surrounding sand is fine and featureless. Their significance,
402 formation and dynamics are still discussed (Liu et al., 2018; Mielck et al., 2015; Murray et al., 2014a;
403 Rosenberger et al., 2019). Some have been attributed to channelized offshore storm-return flows
404 (Pretorius et al., 2018) and they are thought to exhibit positive sorting feedback (Goff et al., 2005;
405 Green et al., 2004; Gutierrez et al., 2005; Murray and Thieler, 2004). Other smaller sediment structures
406 or sediment heterogeneities have also been described on the shoreface, such as ripples or gravel
407 outcrops (Browder and McNinch, 2006; Inman and Adams, 2005; Schupp et al., 2006).

408



409

410 *Figure 4. (colour) Example of sedimentary bedforms (shoreface-connected ridges & sorted bedforms) visible on the*
 411 *bathymetry from Fire Island (USA) (From: Hapke et al., 2016)*

412 In some instances, formation and evolution of superficial sand bodies is linked to the geological
 413 framework. For example, McNinch (2004) and Browder and McNinch (2006) found a correlation
 414 between the presence of palaeochannels and shore oblique sandbars. They postulated that
 415 inhomogeneity in the geological framework could influence the hydrodynamics and that variation in
 416 the nature of the outcropping seafloor could influence the organisation of bedforms. Similarly, Durán
 417 et al. (2018) postulate that irregularities in palaeotopography initiate the formation of and influence
 418 the orientation and distribution of sand ridges.

419 The sedimentary features present on the shoreface can be an indication of the sediment supply
 420 available. Thieler et al. (2014, p. 128) state that ‘where modern sediment is relatively abundant, the
 421 inner shelf contains shoreface-attached ridges and shoal complexes. Where modern sediment is
 422 lacking, the seafloor is characterized by sorted bedforms’. Bedforms and sand bodies, as they develop
 423 and evolve under a specific set of conditions, are morphological indicators of the physical environment
 424 on the shoreface, such as the hydrodynamic climate or the sediment availability. More importantly,
 425 sedimentary features present on the shoreface also seem to influence coastal morphodynamics and
 426 shoreline evolution in many ways (see section 8.3).

427

428 **8. Shoreface morphodynamics**

429 **8.1 Shoreface zonation: Upper/Lower shoreface**

430 The division between upper and lower shoreface morphodynamics is reflected in the notion of depth
431 of closure (and associated wave base) as described by Hallermeier (1981). A number of studies on
432 depth of closure exist in the literature (Birkemeier, 1985; Li et al., 2005; Nicholls et al., 1998, 1997;
433 Robertson et al., 2008), and a selection of studies in contrasting environments are reviewed here.

434 Within a micro-meso tidal environment on the Dutch coast where mean tidal range varied from 1.4m
435 to 1.7m and peak tidal velocity reached 1 ms^{-1} , Hinton and Nicholls (1999) analysed a long-term
436 dataset (20 years) of shoreface profiles to identify the depth of closure for various sections. The
437 observed DoC ranged between 5.0 and 9.2m. Hallermeier's DoC (using a 5-year period) was also
438 calculated, and predicted a DoC at 9.2m. Hinton and Nicholls (1999), however, also observed
439 significant morphological variation seaward of this depth of closure. This morphological variability was
440 only observed over longer time scales ($> 10^1$ years) and at depths greater than 12m. This suggested
441 that the shoreface displays two distinct behaviours occurring at different time scales, highlighting the
442 different behaviour of the upper and lower shoreface zones.

443 In the Mediterranean Sea, a low-energy micro tidal environment, Frihy et al. (2008) examined the
444 seasonal response of the Abu Qir Bay, Egypt, calculating monthly DoC (using Hallereier's formula) and
445 depths of wave base. While the DoC (d_l) varied between 6 and 14m the wave base (d_i) varied between
446 16 and 29m. Maximum d_i varied between 45m in winter and 23m in summer. A previous study (Naffaa
447 et al., 1995) of the DoC that encompassed the same area calculated observed DoC (using historical
448 survey map data) as well as Hallermeier's d_l and d_i . The observed DoC calculated for over 65 years was
449 25m. Naffaa et al. (1995) calculated the d_i with the same 65 years return period and obtained a value
450 of 25.7m using Hallermeier's equation. The Frihy et al. (2008) study of Abu Qir Bay showed seasonal
451 patterns attuned to the wave climate and in particular to the fair/storm weather alternation and, for

452 the same area the work of Naffaa et al. (1995) showed, that the lower shoreface was morphologically
453 active on a multi-decadal time scale ($>10^1$ years).

454 Valiente et al. (2019, 2017) calculated the inner and outer depths of closure, according to various
455 formulations, for the macrotidal, high energy embayments of the coast of Cornwall and Devon (UK)
456 using a 4-year wave time series, giving results ranging between 18.8m and 23.3m for d_l and between
457 33.6m and 50.1m for d_i . Both d_i and d_l decreased from south to north according to the decrease in
458 incoming wave heights. Using nearshore wave conditions obtained through hydrodynamic modelling,
459 Valiente et al. (2019) also looked at spatial variability of the DoC within each embayment as well as
460 the average DoC for each embayment. When compared to observed DoC (obtained from repeated
461 shoreface profiles over a 6-year period at one of the embayment), they found that offshore wave
462 conditions over-estimated the DoC and that the use of wave conditions at the 20m contour returned
463 results more comparable to the observed DoC. Overall their results showed that Hallermeier's DoC
464 (calculated with nearshore wave climate) remains a valid approximation for the identification of the
465 limit of significant seasonal morphological change. They also looked at bed shear stress as an indicator
466 of the boundary for sand motion (DoT, depth of transport; see section 4) and when taking tides into
467 account DoT reaches 30 to 50m for macrotidal Cornwall. This showed that intense sediment transport
468 occurs deeper than previously considered (especially in macrotidal environments) meaning that the
469 volume of reworked and transported sediment on the lower shoreface is most likely to be larger than
470 previously thought and is certainly non-negligible.

471 While both upper and lower shoreface zones are active, it appears that the time scales at which
472 morphological change operates in each zone are significantly different. Further, even if the upper
473 shoreface dynamic is closely linked to nearshore wave conditions, both upper and lower shoreface
474 morphodynamics are the result of the combined effect of multiple drivers and interactions that modify
475 the net shape of the shoreface across different temporal scales.

476 ***8.2 Drivers of shoreface morphology***

477 **8.2.1 Lower shoreface**

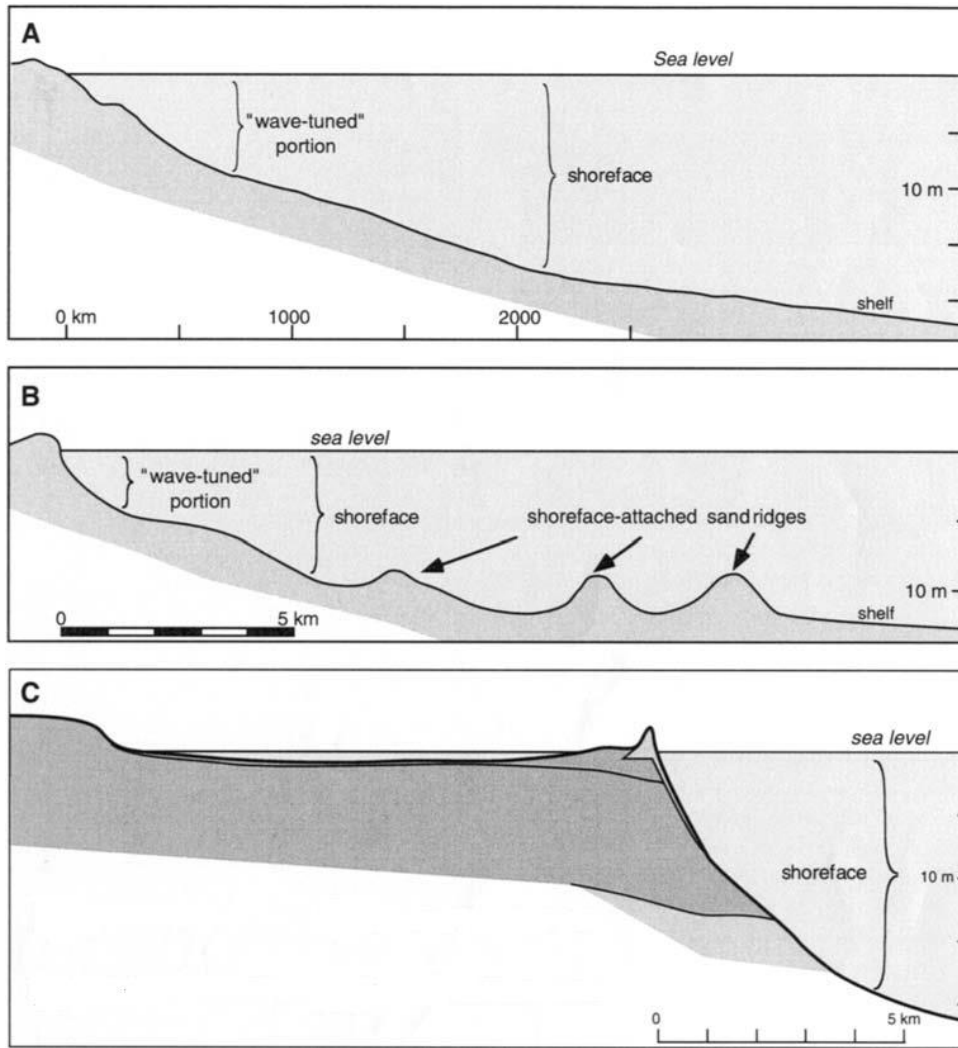
478 Morphological change on the lower shoreface is driven by the effect of waves and currents combined,
479 with most variability occurring during storm events when currents tend to transport sediment from
480 the foreshore/upper shoreface onto the lower shoreface (Niedoroda and Swift, 1981; Niedoroda et
481 al., 1984; Swift et al., 1985; Vincent et al., 1983). As morphological variability on the lower shoreface
482 is relatively small compared to the upper shoreface it is only observable during energetic events or
483 over longer ($> 10^1$ years) time periods. The relative importance of each of the drivers impacting lower
484 shoreface morphodynamics is still relatively unknown. For example, Backstrom et al. (2015; 2000)
485 found different morphological responses to a storm on two adjacent shorefaces on the high energy
486 coast of Northern Ireland despite the storm characteristics being similar for both shorefaces. The
487 difference in response of the two shoreface (accretion was observable on one shoreface whilst only
488 minor changes on the other) was attributed to geological shoreface characteristics such as antecedent
489 morphology, slope and the presence of available sediment (sand bodies). Indeed, for the same event
490 the more dissipative shoreface was only slightly affected while the steeper shoreface, with nearby
491 sand bodies, was significantly more accreted.

492 From the limited set of observations available in the literature, it seems that lower shoreface
493 morphodynamics are influenced both by the hydrodynamic climate and geological factors (i.e.
494 underlying geological framework, sediment supply) reflected in its morphology (**Figure 5**). The relative
495 importance of internal (hydrodynamics) versus external constraints seems to be variable and
496 dependant on the time scale involved, for example external constraints vary with seasonal or inter-
497 annual patterns.

498 There is also marked spatial variability in shoreface morphology and factors such as slope (Aagaard,
499 2014; Bowen, 1980) influence their behaviour. Patterson and Nielsen (2016) examined sand transport
500 on the lower shoreface in the Gold Coast region of western Australia. The site encompassed the
501 sediment-rich lobe of the Nerang River, as well as adjacent shorefaces which are less affected by the

502 local sediment discharge. The long-term evolution (multi-decadal) of the river lobe was interpreted in
503 terms of sediment transport and, as the lobe is in disequilibrium, significant change was observed
504 between 1966 and 2012. Rates of shoreward sand transport from 12.8 m³/m/yr at 18m to 89.1
505 m³/m/yr were calculated and shown to be dependent on wave conditions, as well as water depth and
506 shoreface slope.

507 Through numerical modelling, Preston et al. (2018) investigated the role of slope and wave energy in
508 nearshore morphodynamics. They showed that for an embayed beach, shoreface slope exerted a
509 control on beach recovery. Specifically, they suggest that beaches with steeper shorefaces are less
510 likely to recover from storms than beaches with more gently sloping shorefaces because (p.2429)
511 “bathymetric slope is a major control on the nearshore sediment budget under calm climatic
512 conditions”. However, during storms, hydrodynamics seem to have more control over sediment loss
513 than the slope (Preston et al., 2018).



514

515 **Figure 5.** Diagram of various possible shoreface morphologies (Modified from: Clifton et al., 2005) A: Unconstrained
 516 morphology B: Morphology influenced by sediment features C: Morphology constrained by geologic framework (thin layer of
 517 sand over bedrock)

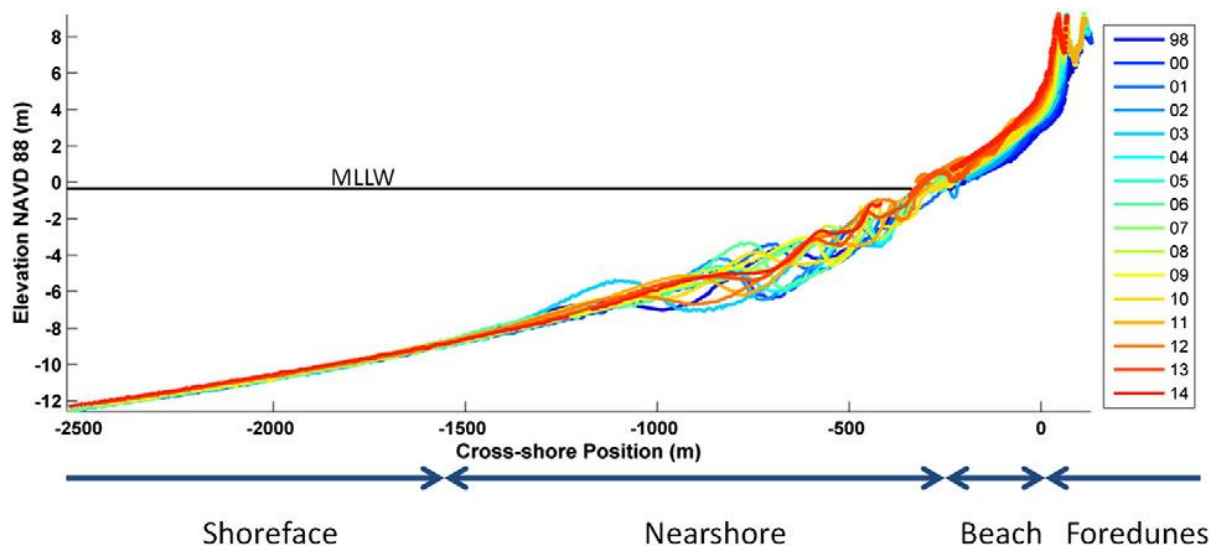
518 **8.2.2 Upper shoreface**

519 As a reminder, we propose to define the 'shoreface' as corresponding with the literature definition of
 520 the lower shoreface, while the 'nearshore' is defined as a combination of the upper shoreface and surf
 521 zone. Although several definitions of the upper shoreface include the (fairweather) surf zone, it is
 522 excluded from consideration here since surf-zone processes are distinctive and different (involving
 523 wave breaking, secondary wave motions, etc.) Sediment transport on the upper shoreface can be
 524 attributed to the temporary extension of the surf zone to the upper shoreface during storm events
 525 (**Figure 6**). Morphological variations of the upper shoreface are thus linked to the dynamics of the
 526 outer surfzone bar and the spatio-temporal variability of the position of the surf zone (Lee et al., 1998;

527 Ruggiero et al., 2016). Antecedent morphology and storm grouping also seem to influence upper
528 shoreface variations. The cumulative effect of successive storms prompts a larger change in upper
529 shoreface morphology because of insufficient recovery between storms.

530 Anthony (2008, p. 243) similarly argued that “Another important aspect of the sediment dynamics of
531 the inner and outer shoreface link is the role of surf zone sediment dynamics in mediating spatial
532 patterns of shoreface elevation change and net losses offshore during storms”. In other words,
533 Anthony (2008) suggests that further potential longshore modulation/variation in morphodynamics
534 due to the influence of the surf zone morphodynamics which due to bars and rip effect etc. has a
535 strong three-dimensional component.

536 Aleman et al. (2015) documented the morphological variability of the coast along the Gulf of Lyon
537 (Mediterranean, France). The depth of closure for the area was calculated at 7.6m and the DoC
538 observed from successive profile surveys varied between 1.4m and 7.4m (Sabatier et al., 2005). Here
539 the DoC gives an indication of the extent of the shoreface that is most affected by changes in incoming
540 wave energy, i.e. the upper shoreface. The offshore distance of the DoC put the morphologically active
541 zone (from shore to depth 7.6m) at distances up to 2.5km offshore for the more dissipative and rock
542 platform-constrained shoreface profiles. Conversely, for reflective shoreface morphologies, the limit
543 of the active zone was less than 200m from the shoreline. This illustrates that a wide array of shoreface
544 configurations can exist for relatively similar offshore wave conditions and tide regimes. It also shows
545 that for different morphologies the extent of the shoreface affected by waves, (the shoaling zone) can
546 vary considerably and with it the stock of sand available for onshore transport.



547 Shoreface Nearshore Beach Foredunes

548 *Figure 6. (colour) Example of profile morphological variability in the Long Beach Peninsula (USA) (From: Ruggiero et al 2016).*
 549 *Each profile corresponds to a survey (one per year from 1980 to 2014).*

550 **8.2.3 . Shoreface sediment supply and exchanges**

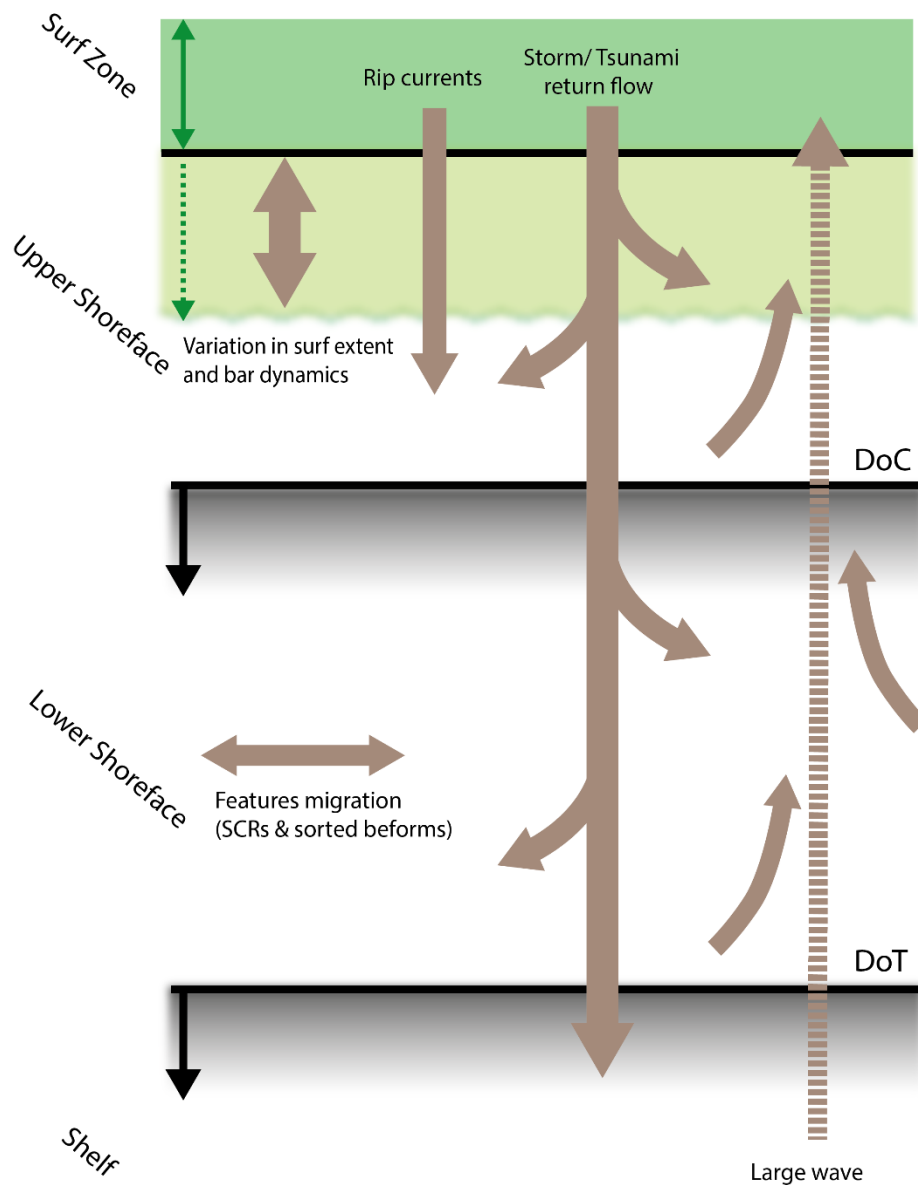
551 Although “long-term observations of shoreface bathymetry change are rare” (Cowell and Kinsela,
 552 2018), sediment transfers to and from the shoreface and within the shoreface itself have been noted
 553 in several studies. These transfers have been linked to multiple spatiotemporally variable processes
 554 which are primarily episodic in nature (Figure 7). Excluding wave and tide-driven sediment motions
 555 (see section 5), the following have been reported:"

- 556 1. Variation in surf zone extent. Periodically, under high wave conditions, the upper shoreface is
 557 affected by surf zone processes, which lead to appreciable changes in bed level. This is
 558 illustrated in the well-known seasonal dynamics of nearshore bars (Aubrey, 1979) and by the
 559 seasonal changes in beach/ surf zone states (Wright and Short, 1984; Wright et al., 1985). For
 560 example, wave breaking typically occurs further offshore during winter than summer. Indeed
 561 large wave events are responsible for transfer of sediment between the shoreface and
 562 surfzone/beach. Often this is evidenced in onshore bar migration at seasonal timescales
 563 (Aagaard et al., 2010, 2004). Offshore bar migration in the surf zone usually ends with bar
 564 disintegration and sediment dispersal at the seaward limit of the surf zone (Shand et al., 1999).

- 565 2. Generation of rip currents. Rip currents that originate in the surf zone can carry sediment
566 offshore and deposit it on the shoreface where it may be sequestered or return shoreward
567 under constructional wave action (Castelle et al., 2016; Loureiro et al., 2012a).
568
- 569 3. Onshore-directed flows during storms. Extreme waves have frequently been documented to
570 transfer shoreface sediment onshore where it is deposited as washover fans (Aagaard and
571 Kroon, 2019). These sediments originate in the surf zone and sites to seaward, including the
572 shoreface (Schwartz, 1975). Recent studies (Pham et al., 2017) also show that some tsunami-
573 generated overwash sediments originated from shallow marine (shoreface) environments.
574 Fruergaard et al. (2013) documented the deposition of large volumes of sand transported
575 from deep water to the shoreface during and after a 1:1000-year storm in the North Sea.
576 Subsequent emergence led to generation of ephemeral spits and barrier islands.
- 577 4. Offshore-directed flows. Following storms (Pretorius et al., 2018; Siringan and Anderson,
578 1994) and tsunami (Richmond et al., 2011; Slooman et al., 2018) deposition of sediment has
579 been recorded on the shoreface. Liu and Goff (2018) documented lobe structures on the
580 stable (prograding) shoreface of Fire Island (New York, USA) that were attributed to storm
581 return flows. Channelized storm return flows have been linked to the formation and
582 maintenance of SCRs (Pretorius et al., 2018).
- 583 5. Longshore sediment movement on the shoreface has recently been documented after storm
584 events, both for sand-rich features and sorted bedforms. For example, on Fire Island's
585 shoreface a retreating area showed erosion and subsequent redistribution of sediment via
586 longshore processes (bedforms migration) while nearby sediment rich areas with SCRs also
587 showed signs of longshore sediment transport (Liu and Goff, 2018). Other studies in the same
588 area also documented bedform migration driven by hurricane events (Goff et al., 2015;
589 Schwab et al., 2017).

- 590 6. Shoreface erosion. Evidence of shoreface-derived sediment in the coastal system is
591 widespread, especially on transgressive shorefaces where underlying rock is periodically
592 exposed and subject to wave erosion (ravinement) (Riggs et al., 1995). Contemporary erosion
593 of bedrock outcrop on the shoreface has recently been documented by repeat side-scan sonar
594 surveys in the Baltic Sea (Schwarzer et al., 2014). This sediment contributes locally to the
595 shoreface sediment budget.
- 596 7. Shoreface nourishment. Experiments with shoreface nourishment have shown that sediment
597 is exchanged between shoreface and surf zone (Grunnet and Ruessink, 2005; Ojeda et al.,
598 2008), but also that the change in morphology created by nourishments in the form of a bar
599 on the shoreface has a shielding effect during energetic conditions (Barnard et al., 2009;
600 Huisman et al., 2019).

601



602

603 *Figure 7: Schematic representation of sediment exchange over the shoreface. With, The surf zone (in dark green) and upper*
 604 *shoreface (light green) are depicted with the upper and lower shoreface limits (solid black lines; see Figure 9) The schematic*
 605 *represents episodic expansion of the surf zone during energetic events. In brown, the arrows depict the sediment transport*
 606 *mechanisms across the shoreface.*

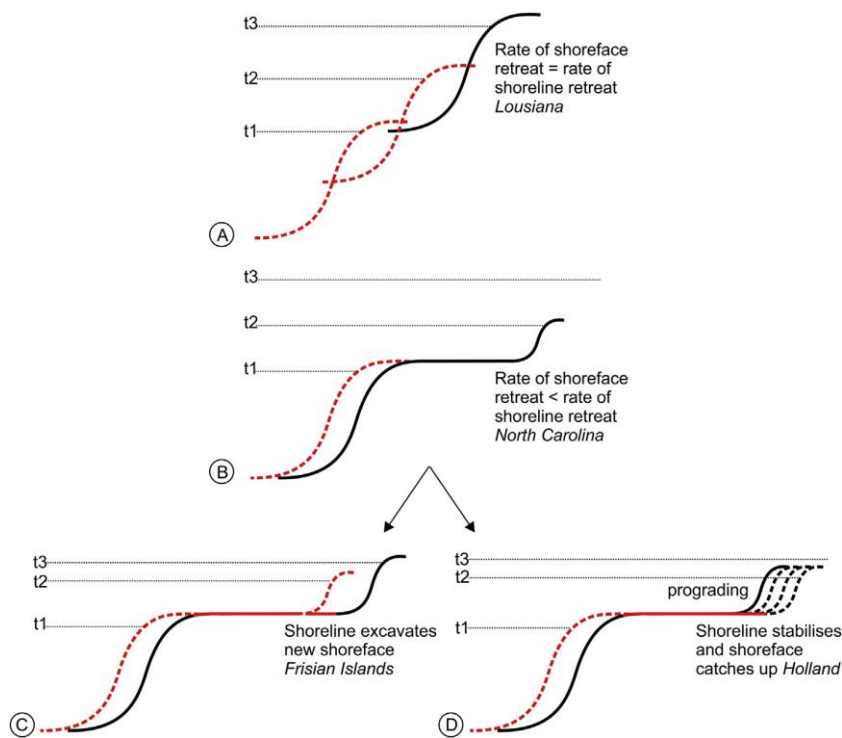
607 **8.2.4 Sea Level Rise**

608 Understanding the response of shoreface morphology and behaviour to sea-level change over decadal
 609 to century timescales (10^1 to 10^2 years) is hampered by the lack of long-term datasets and the difficulty
 610 of isolating the sea-level signature from that of shorter-term dynamic processes, a problem that
 611 persists even on the much more data-rich beach environments (Cooper and Pilkey, 2004). Information
 612 about mesoscale shoreface behaviour is, however, sometimes available from discontinuous historical

613 records (e.g. bathymetric charts) (Cooper and Navas, 2004; Hanna and Cooper, 2002) and, for longer
614 (geological, $>10^2$ years) time scales, seismic and coring data. The dynamics have also been simulated
615 (and sometimes predicted) via models. A wide array of behaviour models has been developed, from
616 statistical- to process-based models that describe shoreface reaction to sea level rise. Early
617 approaches to long-term shoreface evolution assumed time-invariant shoreface profiles (Cowell et al.,
618 1999), while later models allowed for shoreface profile evolution according to the presence of an
619 erodible or non-erodible substrate (Thieler et al., 1995). Some of the most recent studies point to the
620 importance of the slope as a strong control for long term evolution (Ciarletta et al., 2019; Deng and
621 Wu, 2020; Ribó et al., 2020).

622 The conceptual behaviour model for barrier shorefaces as explained by Cooper et al. (2018) describes
623 three modes (keep-up, give-up and catch-up) of shoreface response to sea level rise (**Figure 8**). In this
624 model, the rate of sea-level rise is a key determinant of shoreline behaviour but other internal factors
625 (sediment supply, sediment volume and basement erodibility), also play a role. At mesoscale the
626 geological inheritance dominates shoreface morphology and conditions the response to forcing
627 through sea-level change and storm events. Knowledge of the contribution of shoreface dynamics to
628 the nearshore stratigraphy, and in particular the processes that contribute to development of wave
629 ravinement (erosion) surfaces (Zecchin et al., 2019), has important implications for determination of
630 former sea levels from seismic stratigraphic records as shown by Plets et al. (2019). Shoreface deposits
631 are frequently found in the geological record in preference to beach units. This shows their propensity
632 for preservation by burial or overtopping.

633 The focus of this paper is the mesoscale (10^1 to 10^2 years), there is, however, (despite their
634 propensity for preservation by burial or overstepping) few studies utilizing such deposits to infer the
635 morphodynamics of the shoreface over longer timescales.



636

637 **Figure 8.** (colour) Diagram of barrier-shoreface retreat mode. A. Barrier and shoreface retreat at equal rates (keep-up). B.
 638 Shoreface retreat slower than barrier C&D. Shoreface "catch-up" with t1 t2 t3 the successive stages of sea level rise. From
 639 Cooper et al. (2018)

640

641 **8.3 Shoreface-shoreline interactions**

642 During storm events sediment can be transported offshore to the lower shoreface (Niedoroda et al.,
 643 1984; Preston et al., 2018), and since it is then beyond the depth of closure, it is then considered lost
 644 to the coastal system. However, advances in the study of the role of the shoreface in the coastal
 645 system and sediment budget suggest that shoreface sediment (even beyond the depth of closure)
 646 might in fact play a key role in nearshore morphodynamics. Indeed, several studies (Billy et al., 2013;
 647 Brunel et al., 2014; Lazarus and Murray, 2011; Safak et al., 2017; Schupp et al., 2006; Thomas et al.,
 648 2011; Valvo et al., 2006) have linked shoreline shape and mesoscale variation patterns to adjacent
 649 shoreface setting.

650 Frihy et al. (1991) examined the link between shoreline evolution and nearshore bathymetric change
 651 in the Nile Delta, Egypt, and found no significant relationship between shoreline change and nearshore
 652 (i.e. shoreface) sediment texture, slope or depth. They did, however, attribute erosion and accretion

653 patterns to movement of eroded sediment or sediment from offshore sources, suggesting that the
654 shoreface might contribute to shoreline dynamics.

655 Wijnberg (2002), found no correlation between decadal coastal behaviour and sediment
656 characteristics or offshore hydrodynamics on the Dutch coast but instead linked spatial changes in
657 decadal behaviour to variation in shoreface morphology, especially the presence of “terrace like
658 features” on the shoreface linking shoreface morphology and coastal behaviour. Similarly, Cooper et
659 al. (2004) linked nearshore behaviour to sediment accumulation and associated bathymetric change
660 on the shoreface.

661 Miselis and McNinch (2006), explored the relationship between shoreline variations and nearshore
662 sediment volume in North Carolina, and established that the volume of sediment stored on the
663 shoreface was correlated with decadal shorelines over decadal timescales. Sediment-poor shorefaces
664 were associated with smaller shoreline change rates than sediment-rich shorefaces.

665 The shoreface of Fire Island, has been the subject to multiple studies regarding the role of the
666 shoreface in the coastal system, for example Goff et al. (2015) examined the impact of hurricane Sandy
667 on the shoreface and found that “sand ridges and sorted bedforms appear to act as a regulator of
668 storm-forced erosion of material beneath the modern sand layer” thereby limiting erosion of older
669 sediment as a form of supply of modern sediment available for transport. Hapke et al. (2016), applied
670 statistical analysis to correlate shoreline response of Fire Island with potential controls, especially
671 storm processes and underlying shoreface geology. The correlation analysis suggested (p.52) that:
672 “[long term shoreline] patterns result from an unresolved combination of, or feedback between,
673 storm processes and framework geology (bathymetric variability and sediment availability)”.

674 Fire Island has also been the subject of several studies examining underlying geological control of the
675 area and evidence of onshore-directed sediment transport across the shoreface (Hapke et al., 2010;
676 Schwab et al., 2013, 2000). Those studies show that the shoreface acts as a source and/or a conduit
677 for onshore sediment flux and has a role in foreshore long-term ($>10^1$ years) morphodynamics; there

678 is an apparent link between the volume of shoreface sediment and foreshore behaviour. Safak et al.
679 (2017) subsequently used a three-dimensional, hydrodynamic-based model to examine the effects of
680 shoreface connected sand ridges on shoreline variability at Fire Island. Their results show that
681 hydrodynamic processes and sediment flux are controlled by the effects of offshore geologic
682 framework and that cross-shore flows between the shelf and the coast (i.e. flow on the shoreface)
683 influence coastal evolution and shoreline variability at decadal time scales.

684 In the larger framework of the Mid-Atlantic Bight, McNinch (2004) highlighted a 'suggestive spatial
685 alignment' between shoreline erosional hotspots and shore-oblique bar and associated outcrops. A
686 subsequent study of the same area by Schupp et al. (2006), correlated areas of high shoreline
687 variability with shore-oblique bar and gravel outcrops but with a spatial offset. These observations
688 reinforce the idea that the shoreface morphology (which seems to reflect sediment volume and
689 geological control) constrains or influences foreshore dynamics in some way. Similarly in South
690 Carolina, Denny et al. (2013) linked stable shorelines to adjacent sediment-poor, erosion-resistant
691 shorefaces, whereas the more variable portions of the shoreline occur around portions of the coast
692 rich in sediment and with large sand bodies. Another study (Oakley et al., 2019) on a North-American
693 shoreface (Rhode Island, US) did not find the shoreface sediment volume to be a good predictor of
694 mesoscale shoreline variation, but hypothesize that the alongshore variations in shoreline variation
695 patterns relates to the antecedent morphology of the shoreface and its heterogeneous nature.

696 Shoreface sand bodies have been shown to exert a strong influence on foreshore change. Sand banks
697 have been shown to decay onshore and provide sediment from the shoreface to the beach-dune
698 system (Aagaard et al., 2004; Anthony, 2013; Anthony et al., 2006; Héquette and Aernouts, 2010;
699 Héquette et al., 2013; Thomas et al., 2011; Verwaest et al., 2020). The opposite phenomenon (offshore
700 bar breakdown followed by transport of sediment from the beach to the lower shoreface) has been
701 documented by Aagaard (2011) on the Danish North Sea coast.

702 On a longer time scale ($>10^3$ years), Kinsela et al. (2016) showed through modelling of south-eastern
703 Australian beaches, that the shoreface contributed around 80% of the sand involved in the growth of
704 Holocene strand plains. They suggest that similar processes might still contribute to contemporary
705 shoreline stability. In the same region, Cowell et al. (2001) found that ‘the annual net supply residual
706 (of offshore sand) is cumulative and would grow to exceed the beach-cut/fill volume after only several
707 decades’, supporting the idea that the shoreface can be an important source of foreshore sand in the
708 longer term.

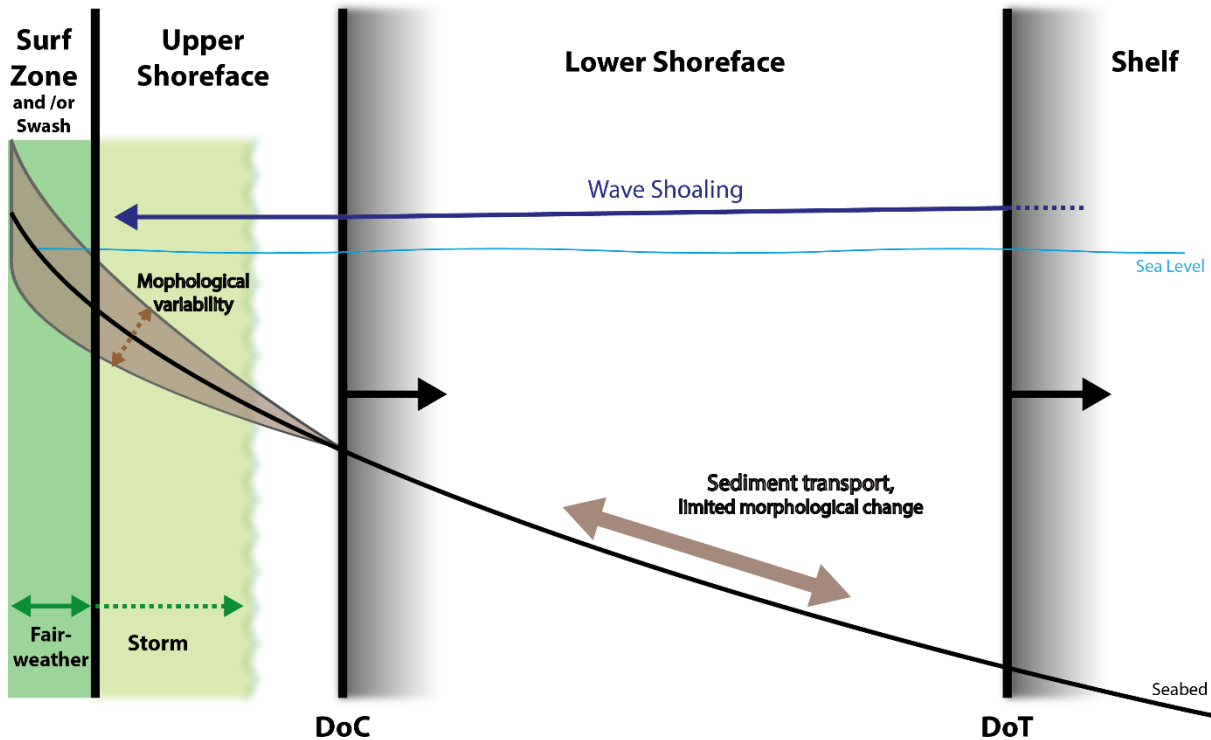
709


710 **9. Discussion**

711 ***9.1 Shoreface definition and morphodynamics***

712 The shoreface is a transition zone between surfzone/beachface and the shelf within which wave
713 shoaling and sediment transport take place. In the face of multiple and conflicting definitions and
714 terminology in the literature, the definition of the shoreface requires standardization. We propose
715 that its landward limit be the outer edge of the surf zone (or the outermost bar) during
716 fairweather/modal conditions, and where this is absent, the seaward edge of the swash zone (or the
717 beach step). This can be justified on the marked difference in nature of wave-driven morphodynamics,
718 pre- and post-breaking. The surf zone is dominated by wave breaking, (and associated processes such
719 as reformation and secondary wave motions or rip currents etc.) (Dally, 2005) and is therefore
720 morphodynamically distinct from the shoreface, not a part of it (**Figure 9**). Although energetic
721 conditions may periodically extend the surf zone seaward, the most persistent process in the upper
722 shoreface is wave shoaling.

Zonation of the Shoreface



723  Offshore migration of limits with timescale

724 *Figure 9: Definition of the shoreface, showing upper and lower shoreface limits. The surf zone is represented in dark green,*
 725 *with light green areas in the upper shoreface representing episodic expansion of the surf zone during energetic events. Brown*
 726 *arrows depict bidirectional movement of sediment in the shoreface and resulting morphological variability.*

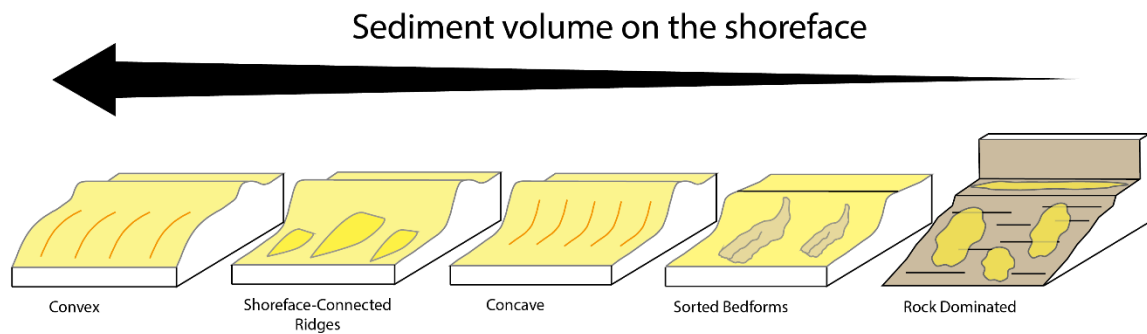
727 The shoreface is made up of two morphodynamically distinct units, namely the upper and lower
 728 shoreface. They are divided by the DoC and the outer limit of the lower shoreface is the threshold at
 729 which waves start to significantly impact the bottom at the mesoscale. We propose to use the Valiente
 730 et al. (2019) depth of transport (DoT) as a calculable boundary for the outer limit of the shoreface at
 731 the mesoscale. Upper and lower shorefaces each exhibit distinctive morphodynamics (**Table 1**). The
 732 shoreface role in adjacent nearshore (surfzone and swash zone) dynamics is manifest in (a)
 733 attenuating waves as they move onshore and (b) as both a sediment source and sink at variable
 734 (largely event-driven) timescales.

735 Upper and Lower shorefaces can be differentiated by their dynamics which play out at different spatio-
 736 temporal scales. Whilst the upper shoreface is active on a short (seasonal) temporal and small spatial
 737 scale ($<10^0$ to 10^1 years and around 10^0 km), the lower shoreface is active over larger scales (10^1 to 10^2

738 years and over 10^1 Km). Because of its mesoscale behaviour, the lower shoreface has often been
739 considered inert and non-influential in terms of coastal dynamics (Hoekstra et al., 1999). The upper
740 shoreface is dominated by wave shoaling and periodic seaward excursions of the surfzone. This is
741 responsible for the morphological variability that occurs on the upper shoreface at seasonal to decadal
742 timescales. The lower shoreface is dominated by oscillatory wave motions that transport sediment
743 but which create morphological change only at long timescales ($>10^1$ years).

744 All shoreface morphodynamic limits exhibit spatio-temporal variability as they can be influenced by
745 water level variations (tides, surges etc.), and variation in storminess with an offshore displacement
746 of the previously cited limits during energetic events, for example. This highlights the interconnectivity
747 between the shoreface zones and adjacent environments. Linkages and overlaps exist between the
748 different zones, particularly at their boundaries. At the junctions between the zones sediment
749 exchanges occur as the boundaries shift. For example, Aagaard (2014) quantified the supply from the
750 lower to the upper shoreface and found it to be coherent with bar migration and aeolian accretion
751 rates. Future targeted research might be able to provide quantifiable limits for the shoreface
752 boundaries based on ratios of morphological change, for example, but thus far, this is not feasible
753 because of the paucity of observations.

754 ***9.2 Sediment supply and shoreface morphology***



755

756 **Figure 10:** Shoreface morphological classification as a function of sediment supply. Typical morphologies associated with,
 757 (increasing) sediment volume on the shoreface from a sediment starved erosive (far right) shoreface to a prograding
 758 shoreface (far left) with intermediate morphologies indicating the augmentation of available shoreface sediment.

759 The literature shows that a wide variety of shoreface morphologies exist in nature (Athanasidou et al.,
 760 2019; Kinsela et al., 2020). It is unlikely these variations are linked solely to variations in wave
 761 conditions. One of the major factors controlling this variability in morphology seems to be sediment
 762 supply (or availability) and more specifically, the sedimentary bedforms associated with sediment-
 763 poor and sediment-rich shorefaces. Bedforms are an indicator of the presence (or deficit) of sediment
 764 on the shoreface. Offshore of Fire Island (Locker et al., 2017; Schwab et al., 2017) increasing sediment
 765 abundance is reflected in the successive development of sorted bedforms and SCRs. Banks, ridges and
 766 similar features are indicators of sediment-rich areas while sorted bedforms are more typical of
 767 sediment-depleted areas. For example, some shoreface attached sand ridges have been determined
 768 to originate from relict tidal deltas (McBride and Moslow, 1991) supporting the hypothesis that these
 769 features originate in sediment-rich areas.

770 We propose a tentative classification of shoreface morphologies based on increasing sediment
 771 abundance (**Figure 10**). Shorefaces that lack sediment are likely to be much more erosional. With the
 772 addition of a limited amount of sediment, sorted bedforms develop with underlying lag deposits
 773 exposed between sandy areas of positive relief. Increased sediment supply can then lead to
 774 development of SCRs either from relict sediment sources (e.g. submerged ebb deltas) or

775 contemporary inputs. Evidence of the link is present in the longshore variation in shoreface
776 morphology offshore of Fire Island, for example where onshore sediment abundance and accretion is
777 mirrored by offshore SCRs at the downdrift limit of the barrier. We surmise that increased sediment
778 abundance ultimately creates convex shoreface morphologies. At longer timescales ($>10^1$ to 10^1 years)
779 shorefaces might evolve along this spectrum according to whether sediment supply is abundant or
780 absent (Deaton et al., 2017; Raff et al., 2018; Shawler et al., 2019). The equilibrium shoreface profile
781 in this conceptual scheme is one of a spectrum of possible morphologies.

782 The influence of shoreface morphology on the overall mesoscale coastal morphodynamics, however,
783 is still unclear, especially in terms of its contribution to the overall sediment budget. While in some
784 locations the shoreface acts as a net sediment source (Denny et al., 2013; Ruggiero et al., 2016;
785 Verwaest et al., 2020), for other regions it seems to be a sink (Aagaard, 2011; Finkl, 2004). It is clear,
786 however, that sediment exchanges within and between the shoreface and adjacent environments is
787 strongly episodic and likely strongly influenced by geological setting (sediment supply and antecedent
788 topography). In addition to the implicit geological control on such exchanges, these sediment transfers
789 are likely to be spatially and temporally variable. Whilst the impact of the variable shoreface
790 morphologies on the foreshore is still not fully understood, several studies have established links to
791 observed behavioural shoreline patterns, demonstrating the potential importance of shoreface
792 morphology to the overall coastal dynamics (Latapy et al., 2020; Verwaest et al., 2020; Wijnberg,
793 2002). Unfortunately, the paucity of datasets of shoreface morphology, preclude detailed insights into
794 the mesoscale dynamics of these shoreface morphologies and the adjacent coasts.

795 The evidence shows that the shoreface is morphodynamically distinct but it does play an important
796 role in nearshore sediment exchanges and is an important conditioner of processes in the surfzone
797 and landward.

798 ***9.3 Future challenges and opportunities***

799 The field of coastal geoscience has developed around the principle of equilibrium, with the first
800 mention of equilibrium profile dating as far back as the early 19th century (Fenneman, 1902). Since
801 then, research on coastal morphology and processes has mostly been focused on the beach and surf
802 zone through which the dynamic principles that control beach and surf zone morphology have been
803 developed. The Wright and Short (1984) model, which classifies beach state on a spectrum ranging
804 from reflective to dissipative according to their morphology, was subsequently refined and adapted
805 to account for further driving factors such as tides (Jackson et al., 2005; Loureiro et al., 2013; Masselink
806 and Short, 1993; Short and Jackson, 2013)

807 Whereas the drivers of beach morphology have been well–constrained, the same is not true of the
808 shoreface, possibly because of the gap in both spatial and temporal data that once existed. Spatial
809 data availability is now being considerably enhanced by technical advances in data acquisition but the
810 spatiotemporal scale at which shoreface dynamics operate still poses problems for empirical studies.

811 Much in the same way as for beaches and surf zones the shoreface can assume a spectrum of forms
812 (Kinsela et al., 2020) that do not result from just grain size and wave climate forcing but rather a
813 multiplicity of factors. Such a conceptual model would help create a much more realistic
814 representation of existing shoreface morphologies worldwide.

815 Our proposed shoreface classification based on sediment supply provides one model that may prove
816 to be universally applicable and could serve to coordinate studies focusing on very different
817 spatiotemporal scales. Future approaches to understanding shoreface dynamics should consider this
818 and the diverse factors that ultimately influence them at meso- and geological scales. This will improve
819 scientific, engineering and management understanding of shoreface dynamics *per se* as well as add
820 important new insights into their association with beach and shoreline behaviour.

821 **Acknowledgements**

822 This work was supported through funding from a DfE International research Award to Klervi Hamon-
823 Kerivel. This work was also supported by ISblue project, Interdisciplinary graduate school for the blue
824 planet (ANR-17-EURE-0015) and co-funded by a grant from the French government under the program
825 "Investissements d'Avenir". It is a contribution to NERC project NE/H024301/1 "Late Glacial sea level
826 minima".

827

828 Declarations of interest: none

829

	Upper Shoreface		Lower Shoreface	
Limits	Fairweather Surf/Swash zone	Morphologically active zone	Long-term intense transport	limit of sediment
Calculation		Hallermeier's DoC	Valiente's DoT	
Characteristic time scale of morphodynamics	Seasonal to annual 10^0 years		Mesoscale > 10^1 years	
Main drivers of morphology	Hydrodynamics (wave, wind, tide...)		Sediment supply/availability/size Geological framework & morphology	
Hydrodynamics	Wave shoaling, and wave breaking during storm conditions		Wave shoaling	
Other drivers of the morphology	Geology & sediments		Hydrodynamics	
	Antecedent morphology, slope Storm grouping, ocean patterns Biological processes			

831 *Table 1. Major characteristics of shoreface components.*

832

833

834

835 Aagaard, T., 2011. Sediment transfer from beach to shoreface: The sediment budget of an
836 accreting beach on the Danish North Sea Coast. *Geomorphology* 135, 143–157.
837

838 Aagaard, T., 2014. Sediment supply to beaches: cross-shore sand transport on the lower
839 shoreface. *Journal of Geophysical Research: Earth Surface* 119, 913–926.
840

841 Aagaard, T., Davidson-Arnott, R., Greenwood, B., Nielsen, J., 2004. Sediment supply from
842 shoreface to dunes: linking sediment transport measurements and long-term morphological
843 evolution. *Geomorphology* 60, 205–224.
844

845 Aagaard, T., Greenwood, B., Hughes, M., 2013. Sediment transport on dissipative,
846 intermediate and reflective beaches. *Earth-science reviews* 124, 32–50.
847

848 Aagaard, T., Kroon, A., 2019. Decadal behaviour of a washover fan, Skallingen Denmark.
849 *Earth Surface Processes and Landforms* 44, 1755–1768.
850

851 Aagaard, T., Kroon, A., Greenwood, B., Hughes, M.G., 2010. Observations of offshore bar
852 decay: Sediment budgets and the role of lower shoreface processes. *Continental Shelf
853 Research* 30, 1497–1510.
854

855 Aleman, N., Robin, N., Certain, R., Anthony, E., Barusseau, J.-P., 2015. Longshore
856 variability of beach states and bar types in a microtidal, storm-influenced, low-energy
857 environment. *Geomorphology* 241, 175–191.
858

859 Anthony, E.J., 2008. A Medium-Term (Meso-scale) Approach to Beach and Barrier
860 Processes, in: *Shore Processes and Their Palaeoenvironmental Applications*. Elsevier, pp.
861 241–261.
862

863 Anthony, E.J., 2013. Storms, shoreface morphodynamics, sand supply, and the accretion and
864 erosion of coastal dune barriers in the southern North Sea. *Geomorphology* 199, 8–21.
865

866 Anthony, E.J., Vanhee, S., Ruz, M.-H., 2006. Short-term beach-dune sand budgets on the
867 north sea coast of France: Sand supply from shoreface to dunes, and the role of wind and
868 fetch. *Geomorphology* 81, 316–329.
869

870 Aragonés, L., Pagán, J., López, I., Navarro-González, F., Villacampa, Y., 2019. Galerkin's
871 formulation of the finite elements method to obtain the depth of closure. *Science of The
872 Total Environment* 660, 1256–1263.
873

874 Aragonés, L., Pagán, J.I., López, I., Serra, J.C., 2018. Depth of closure: New calculation
875 method based on sediment data. *International Journal of Sediment Research* 33, 198–207.
876

877 Athanasiou, P., Van Dongeren, A., Giardino, A., Vousdoukas, M., Gaytan-Aguilar, S.,
878 Ranasinghe, R., 2019. Global distribution of nearshore slopes with implications for coastal
879 retreat. *Earth system science data* 11, 1515–1529.
880

881 Aubrey, D.G., 1979. Seasonal patterns of onshore/offshore sediment movement. *Journal of
882 Geophysical Research: Oceans* 84, 6347–6354.
883

884 Austin, M., Masselink, G., O'Hare, T., Russell, P., 2009. Onshore sediment transport on a
885 sandy beach under varied wave conditions: Flow velocity skewness, wave asymmetry or
886 bed ventilation? *Marine Geology* 259, 86–101.
887

888 Backstrom, J., Jackson, D., Cooper, A., Loureiro, C., 2015. Contrasting geomorphological
889 storm response from two adjacent shorefaces. *Earth Surface Processes and Landforms* 40,
890 2112–2120.
891

892 Backstrom, J., Jackson, D., Cooper, J., 2007. Shoreface dynamics of two high-energy beaches
893 in Northern Ireland. *Journal of Coastal Research* 50, 594–8.
894

895 Bakker, A., Brinkkemper, J., Steen, F., Tissier, M., Ruessink, B., 2016. Cross-shore sand
896 transport by infragravity waves as a function of beach steepness. *Journal of Geophysical*
897 *Research: Earth Surface* 121, 1786–1799.
898

899 Barnard, P., Erikson, L.H., Hansen, J., 2009. Monitoring and modeling shoreline response
900 due to shoreface nourishment on a high-energy coast. *Journal of Coastal Research* 29–33.
901

902 Bertin, X., de Bakker, A., Van Dongeren, A., Coco, G., Andre, G., Arduin, F., Bonneton, P.,
903 Bouchette, F., Castelle, B., Crawford, W.C., others, 2018. Infragravity waves: From
904 driving mechanisms to impacts. *Earth-Science Reviews* 177, 774–799.
905

906 Billy, J., Robin, N., Certain, R., Hein, C., Berné, S., 2013. Barrier shoreline evolution
907 constrained by shoreface sediment reservoir and substrate control: The Miquelon-Langlade
908 Barrier, NW Atlantic. *Journal of Coastal Research* 65, 2089–2094.
909

910 Bird, E., 1985. *Coastline Changes: a Global Review*. Wiley.
911

912 Birkemeier, W.A., 1985. Field data on seaward limit of profile change. *Journal of Waterway,*
913 *Port, Coastal, and Ocean Engineering* 111, 598–602.
914

915 Boon, J.D., Green, M.O., 1988. Caribbean beach-face slopes and beach equilibrium profiles.
916 *Coastal Engineering Proceedings* 1, 1618–1630.
917

918 Bowen, A., 1980. Simple models of nearshore sedimentation: Beach profiles and longshore
919 bars, in: S.B. McCann (Ed.), *The Coastline of Canada*. Geological Survey of Canada, pp.
920 1–11.
921

922 Browder, A.G., McNinch, J.E., 2006. Linking framework geology and nearshore
923 morphology: correlation of paleo-channels with shore-oblique sandbars and gravel
924 outcrops. *Marine Geology* 231, 141–162.
925

926 Brunel, C., Certain, R., Sabatier, F., Robin, N., Barusseau, J., Aleman, N., Raynal, O., 2014.
927 20th century sediment budget trends on the Western Gulf of Lions shoreface (France): An
928 application of an integrated method for the study of sediment coastal reservoirs.
929 *Geomorphology* 204, 625–637.
930

931 Calvete, D., Falqués, A., De Swart, H., Walgreen, M., 2001a. Modelling the formation of
932 shoreface-connected sand ridges on storm-dominated inner shelves. *Journal of Fluid*

933 Mechanics 441, 169–193.
934
935 Calvete, D., Walgreen, M., Swart, H. de, Falqués, A., 2001b. A model for sand ridges on the
936 shelf: Effect of tidal and steady currents. *Journal of Geophysical Research: Oceans* 106,
937 9311–9325.
938
939 Castelle, B., Scott, T., Brander, R., McCarroll, R., 2016. Rip current types, circulation and
940 hazard. *Earth-Science Reviews* 163, 1–21.
941
942 Ciarletta, D.J., Lorenzo-Trueba, J., Ashton, A., 2019. Mechanism for retreating barriers to
943 autogenically form periodic deposits on continental shelves. *Geology* 47, 239–242.
944
945 Clifton, H.E., 2005. Shoreface, in: *Encyclopedia of Coastal Science*. Springer, pp. 877–881.
946
947 Cooper, J., Jackson, D., Navas, F., McKenna, J., Malvarez, G., 2004. Identifying storm
948 impacts on an embayed, high-energy coastline: examples from western Ireland. *Marine*
949 *Geology* 210, 261–280.
950
951 Cooper, J., Navas, F., 2004. Natural bathymetric change as a control on century-scale
952 shoreline behavior. *Geology* 32, 513–516.
953
954 Cooper, J.A.G., Green, A.N., Loureiro, C., 2018. Geological constraints on mesoscale coastal
955 barrier behaviour. *Global and Planetary Change* 168, 15–34.
956
957 Cooper, J.A.G., Pilkey, O.H., 2004. Sea-level rise and shoreline retreat: time to abandon the
958 Bruun Rule. *Global and Planetary change* 43, 157–171.
959
960 Cowell, P., Hanslow, D., Meleo, J., 1999. The shoreface. *Handbook of beach and shoreface*
961 *morphodynamics* 3, 39–71.
962
963 Cowell, P., Roy, P., Jones, R., 1995. Simulation of large-scale coastal change using a
964 morphological behaviour model. *Marine Geology* 126, 45–61.
965
966 Cowell, P.J., Kinsela, M.A., 2018. Shoreface controls on barrier evolution and shoreline
967 change, in: *Barrier Dynamics and Response to Changing Climate*. Springer, pp. 243–275.
968
969 Cowell, P.J., Stive, M.J., Roy, P.S., Kaminsky, G.M., Buijsman, M.C., Thom, B.G., Wright,
970 L.D., 2001. Shoreface sand supply to beaches, in: *Coastal Engineering 2000*. pp. 2495–
971 2508.
972
973 Dally, W., 2005. Surf zone processes. *Encyclopedia of coastal science* 18, 929–935.
974
975 Dashtgard, S.E., Gingras, M.K., MacEachern, J.A., 2009. Tidally modulated shorefaces.
976 *Journal of Sedimentary Research* 79, 793–807.
977
978 Dashtgard, S.E., MacEachern, J.A., Frey, S.E., Gingras, M.K., 2012. Tidal effects on the
979 shoreface: towards a conceptual framework. *Sedimentary Geology* 279, 42–61.
980

981 Dean, R., 1977. Equilibrium beach profiles: US Atlantic and Gulf coasts. Newark, University
982 of Delaware. Ocean Engineering Report No 12, 151–165.
983

984 Dean, R.G., 1991. Equilibrium beach profiles: characteristics and applications. *Journal of*
985 *Coastal Research* 7, 53–84.
986

987 Deaton, C.D., Hein, C.J., Kirwan, M.L., 2017. Barrier island migration dominates
988 ecogeomorphic feedbacks and drives salt marsh loss along the Virginia Atlantic Coast,
989 USA. *Geology* 45, 123–126.
990

991 Deng, J., Wu, J., 2020. Assessing the effects of shoreface profile concavity on long-term
992 shoreline changes: an exploratory study *Geo-Marine Letters*.
993

994 Denny, J.F., Schwab, W.C., Baldwin, W.E., Barnhardt, W.A., Gayes, P.T., Morton, R.A.,
995 Warner, J.C., Driscoll, N.W., Voulgaris, G., 2013. Holocene sediment distribution on the
996 inner continental shelf of northeastern South Carolina: implications for the regional
997 sediment budget and long-term shoreline response. *Continental Shelf Research* 56, 56–70.
998

999 Durán, R., Guillén, J., Rivera, J., Lobo, F., Muñoz, A., Fernández-Salas, L., Acosta, J., 2018.
1000 Formation, evolution and present-day activity of offshore sand ridges on a narrow, tideless
1001 continental shelf with limited sediment supply. *Marine Geology* 397, 93–107.
1002

1003 Falques, A., Calvete, D., De Swart, H., Dodd, N., 1999. Morphodynamics of shoreface-
1004 connected ridges, in: *Coastal Engineering 1998*. pp. 2851–2864.
1005

1006 Fenneman, N.M., 1902. Development of the profile of equilibrium of the subaqueous shore
1007 terrace. *The Journal of Geology* 10, 1–32.
1008

1009 Finkl, C.W., 2004. Leaky valves in littoral sediment budgets: loss of nearshore sand to deep
1010 offshore zones via chutes in barrier reef systems, southeast coast of Florida, USA. *Journal*
1011 *of Coastal Research* 20, 605–611.
1012

1013 Frihy, O., Nasr, S., Ahmed, M., El Raey, M., 1991. Temporal shoreline and bottom changes
1014 of the inner continental shelf off the Nile Delta, Egypt. *Journal of Coastal Research* 7,
1015 465–475.
1016

1017 Frihy, O.E., Hassan, M.S., Deabes, E.A., Abd El Moniem, A.B., 2008. Seasonal wave
1018 changes and the morphodynamic response of the beach-inner shelf of Abu Qir Bay,
1019 Mediterranean coast, Egypt. *Marine Geology* 247, 145–158.
1020

1021 Fruergaard, M., Andersen, T.J., Johannessen, P.N., Nielsen, L.H., Pejrup, M., 2013. Major
1022 coastal impact induced by a 1000-year storm event. *Scientific reports* 3, 1–7.
1023

1024 Gallop, S.L., Kennedy, D.M., Loureiro, C., Naylor, L.A., Muñoz-Pérez, J.J., Jackson, D.W.,
1025 Fellowes, T.E., 2020. Geologically controlled sandy beaches: Their geomorphology,
1026 morphodynamics and classification. *Science of the Total Environment* 139123.
1027

1028 George, D.A., Hill, P.S., 2008. Wave climate, sediment supply and the depth of the sand-mud
1029 transition: a global survey. *Marine Geology* 254, 121–128.
1030

- 1031 Goff, J.A., Flood, R.D., Austin Jr, J.A., Schwab, W.C., Christensen, B., Browne, C.M.,
 1032 Denny, J.F., Baldwin, W.E., 2015. The impact of Hurricane Sandy on the shoreface and
 1033 inner shelf of Fire Island, New York: Large bedform migration but limited erosion.
 1034 *Continental Shelf Research* 98, 13–25.
 1035
- 1036 Goff, J.A., Mayer, L.A., Traykovski, P., Buynevich, I., Wilkens, R., Raymond, R., Glang, G.,
 1037 Evans, R.L., Olson, H., Jenkins, C., 2005. Detailed investigation of sorted bedforms, or
 1038 “rippled scour depressions,” within the Martha’s Vineyard Coastal Observatory,
 1039 Massachusetts. *Continental Shelf Research* 25, 461–484.
 1040
- 1041 Goodwin, I.D., Freeman, R., Blackmore, K., 2013. An insight into headland sand bypassing
 1042 and wave climate variability from shoreface bathymetric change at Byron Bay, New South
 1043 Wales, Australia. *Marine Geology* 341, 29–45.
 1044
- 1045 Green, M.O., Vincent, C.E., Trembanis, A.C., 2004. Suspension of coarse and fine sand on a
 1046 wave-dominated shoreface, with implications for the development of rippled scour
 1047 depressions. *Continental Shelf Research* 24, 317–335.
 1048
- 1049 Grunnet, N.M., Ruessink, B., 2005. Morphodynamic response of nearshore bars to a
 1050 shoreface nourishment. *Coastal Engineering* 52, 119–137.
 1051
- 1052 Guerrero, Q., Guillén, J., Durán, R., Urgeles, R., 2018. Contemporary genesis of sand ridges
 1053 in a tideless erosional shoreface. *Marine Geology* 395, 219–233.
 1054
- 1055 Guisado-Pintado, E., Jackson, D.W., 2018. Multi-scale variability of storm Ophelia 2017:
 1056 The importance of synchronised environmental variables in coastal impact. *Science of The*
 1057 *Total Environment* 630, 287–301.
 1058
- 1059 Guisado-Pintado, E., Jackson, D.W., 2019. Coastal impact from high-energy events and the
 1060 importance of concurrent forcing parameters: the cases of Storm Ophelia (2017) and Storm
 1061 Hector (2018) in NW Ireland. *Frontiers in Earth Science* 7, 190.
 1062
- 1063 Gutierrez, B.T., Voulgaris, G., Thielier, E.R., 2005. Exploring the persistence of sorted
 1064 bedforms on the inner-shelf of Wrightsville Beach, North Carolina. *Continental Shelf*
 1065 *Research* 25, 65–90.
 1066
- 1067 Hallermeier, R.J., 1978. Uses for a calculated limit depth to beach erosion, in: *Coastal*
 1068 *Engineering* 1978. pp. 1493–1512.
 1069
- 1070 Hallermeier, R.J., 1981. A profile zonation for seasonal sand beaches from wave climate.
 1071 *Coastal engineering* 4, 253–277.
 1072
- 1073 Hampson, G.J., Storms, J.E., 2003. Geomorphological and sequence stratigraphic variability
 1074 in wave-dominated, shoreface-shelf parasequences. *Sedimentology* 50, 667–701.
 1075
- 1076 Hanna, J.E., Cooper, J., 2002. Mesoscale morphological changes on linear, nearshore
 1077 sandbanks, Co. Wexford, SE Ireland. *Journal of Coastal Research* SI 36, 356–364.
 1078
- 1079 Hapke, C.J., Lentz, E.E., Gayes, P.T., McCoy, C.A., Hehre, R., Schwab, W.C., Williams,
 1080 S.J., 2010. A review of sediment budget imbalances along Fire Island, New York: can

1081 nearshore geologic framework and patterns of shoreline change explain the deficit? *Journal*
1082 *of Coastal Research* 26, 510–522.

1083

1084 Hapke, C.J., Plant, N.G., Henderson, R.E., Schwab, W.C., Nelson, T.R., 2016. Decoupling
1085 processes and scales of shoreline morphodynamics. *Marine Geology* 381, 42–53.

1086

1087 Héquette, A., Aernouts, D., 2010. The influence of nearshore sand bank dynamics on
1088 shoreline evolution in a macrotidal coastal environment, Calais, Northern France.
1089 *Continental Shelf Research* 30, 1349–1361.

1090

1091 Héquette, A., Anthony, E.J., Ruz, M.-H., Maspataud, A., Aernouts, D., Hemdane, Y., 2013.
1092 The influence of nearshore sand banks on coastal hydrodynamics and sediment transport,
1093 northern coast of France, in: *Proceedings Coastal Dynamics*. pp. 801–810.

1094

1095 Héquette, A., Desrosiers, M., Hill, P.R., Forbes, D.L., 2001. The influence of coastal
1096 morphology on shoreface sediment transport under storm-combined flows, Canadian
1097 Beaufort Sea. *Journal of Coastal Research* 17, 507–516.

1098

1099 Héquette, A., Hemdane, Y., Anthony, E.J., 2008a. Sediment transport under wave and current
1100 combined flows on a tide-dominated shoreface, northern coast of France. *Marine geology*
1101 249, 226–242.

1102

1103 Héquette, A., Hemdane, Y., Anthony, E.J., 2008b. Determination of sediment transport paths
1104 in macrotidal shoreface environments: a comparison of grain-size trend analysis with near-
1105 bed current measurements. *Journal of Coastal Research* 24, 695–707.

1106

1107 Héquette, A., Hill, P.R., 1993. Storm-generated currents and offshore sediment transport on a
1108 sandy shoreface, Tibjak Beach, Canadian Beaufort Sea. *Marine geology* 113, 283–304.

1109

1110 Hinton, C., Nicholls, R.J., 1999. Spatial and temporal behaviour of depth of closure along the
1111 Holland coast, in: *Coastal Engineering 1998*. pp. 2913–2925.

1112

1113 Hoekstra, P., Houwman, K., Ruessink, G., 1999. The role and time scale of cross-shore
1114 sediment exchange for a barrier island shoreface, in: *Coastal Sediments*. pp. 519–534.

1115

1116 Howell, J.A., Skorstad, A., MacDonald, A., Fordham, A., Flint, S., Fjellvoll, B., Manzocchi,
1117 T., 2008. Sedimentological parameterization of shallow-marine reservoirs. *Petroleum*
1118 *Geoscience* 14, 17–34.

1119

1120 Huisman, B., Walstra, D.-J., Radermacher, M., De Schipper, M., Ruessink, G., 2019.
1121 Observations and modelling of shoreface nourishment behaviour. *Journal of Marine*
1122 *Science and Engineering* 7, 59.

1123

1124 Inman, D.L., Adams, P.N., 2005. Bedforms and closure depth on equilibrium beaches.
1125 *Scripps Institution of Oceanography, Technical Report*.

1126

1127 Jackson, D., Cooper, J., Del Rio, L., 2005. Geological control of beach morphodynamic state.
1128 *Marine Geology* 216, 297–314.

1129

1130 King, E., Conley, D., Masselink, G., Leonardi, N., McCarroll, R., Scott, T., 2019. The impact
1131 of waves and tides on residual sand transport on a sediment-poor, energetic, and
1132 macrotidal continental shelf. *Journal of Geophysical Research: Oceans* 124, 4974–5002.
1133

1134 Kinsela, M.A., Daley, M.J., Cowell, P.J., 2016. Origins of Holocene coastal strandplains in
1135 Southeast Australia: Shoreface sand supply driven by disequilibrium morphology. *Marine*
1136 *Geology* 374, 14–30.
1137

1138 Kinsela, M.A., Hanslow, D.J., Carvalho, R.C., Linklater, M., Ingleton, T.C., Morris, B.D.,
1139 Allen, K.M., Sutherland, M.D., Woodroffe, C.D., 2020. Mapping the Shoreface of Coastal
1140 Sediment Compartments to Improve Shoreline Change Forecasts in New South Wales,
1141 Australia. *Estuaries and coasts* 1–27.
1142

1143 Kraus, N.C., Harikai, S., 1983. Numerical model of the shoreline change at Oarai Beach.
1144 *Coastal Engineering* 7, 1–28.
1145

1146 Larson, M., Kraus, N.C., Wise, R.A., 1999. Equilibrium beach profiles under breaking and
1147 non-breaking waves. *Coastal Engineering* 36, 59–85.
1148

1149 Latapy, A., Héquette, A., Nicolle, A., Pouvreau, N., 2020. Influence of shoreface
1150 morphological changes since the 19th century on nearshore hydrodynamics and shoreline
1151 evolution in Wissant Bay (northern France). *Marine Geology* 422, 106095.
1152

1153 Lazarus, E.D., Murray, A.B., 2011. An integrated hypothesis for regional patterns of
1154 shoreline change along the Northern North Carolina Outer Banks, USA. *Marine Geology*
1155 281, 85–90.
1156

1157 Lee, G., Nicholls, R.J., Birkemeier, W.A., 1998. Storm-driven variability of the beach-
1158 nearshore profile at Duck, North Carolina, USA, 1981-1991. *Marine geology* 148, 163–
1159 177.
1160

1161 Li, Y., Lark, M., Reeve, D., 2005. Multi-scale variability of beach profiles at Duck: a wavelet
1162 analysis. *Coastal Engineering* 52, 1133–1153.
1163

1164 Liu, S., Goff, J.A., 2018. Lower shoreface seismic stratigraphy and morphology off Fire
1165 Island, New York: Evidence for lobate progradation and linear erosion. *Continental Shelf*
1166 *Research* 163, 23–34.
1167

1168 Liu, S., Goff, J.A., Flood, R.D., Christensen, B., Austin Jr, J.A., 2018. Sorted bedforms off
1169 Western Long Island, New York, USA: Asymmetrical morphology and twelve-year
1170 migration record. *Sedimentology* 65, 2202–2222.
1171

1172 Locker, S.D., Miselis, J.L., Buster, N.A., Hapke, C.J., Wadman, H.M., McNinch, J.E., Forde,
1173 A.S., Stalk, C.A., 2017. Nearshore sediment thickness, Fire Island, New York. US
1174 Geological Survey Open-File Report 1024, 21.
1175

1176 Loureiro, C., Ferreira, Ó., Cooper, J.A.G., 2012a. Extreme erosion on high-energy embayed
1177 beaches: influence of megarips and storm grouping. *Geomorphology* 139, 155–171.
1178

- 1179 Loureiro, C., Ferreira, Ó., Cooper, J.A.G., 2012b. Geologically constrained morphological
1180 variability and boundary effects on embayed beaches. *Marine Geology* 329, 1–15.
1181
- 1182 Loureiro, C., Ferreira, Ó., Cooper, J.A.G., 2013. Applicability of parametric beach
1183 morphodynamic state classification on embayed beaches. *Marine Geology* 346, 153–164.
1184
- 1185 Madricardo, F., Rizzetto, F., 2018. Shallow coastal landforms, in: *Submarine*
1186 *Geomorphology*. Springer, pp. 161–183.
1187
- 1188 Masselink, G., Short, A.D., 1993. The effect of tide range on beach morphodynamics and
1189 morphology: a conceptual beach model. *Journal of Coastal Research* 785–800.
1190
- 1191 McBride, R.A., Moslow, T.F., 1991. Origin, evolution, and distribution of shoreface sand
1192 ridges, Atlantic inner shelf, USA. *Marine Geology* 97, 57–85.
1193
- 1194 McNinch, J.E., 2004. Geologic control in the nearshore: shore-oblique sandbars and shoreline
1195 erosional hotspots, Mid-Atlantic Bight, USA. *Marine Geology* 211, 121–141.
1196
- 1197 Menier, D., Estournès, G., Mathew, M.J., Ramkumar, M., Briend, C., Siddiqui, N., Traini, C.,
1198 Pian, S., Labeyrie, L., 2016. Relict geomorphological and structural control on the coastal
1199 sediment partitioning, North of Bay of Biscay. *Zeitschrift für Geomorphologie* 60, 67–74.
1200
- 1201 Menier, D., Mathew, M., Cherfils, J.-B., Ramkumar, M., Estournès, G., Koch, M.,
1202 Guillocheau, F., Sedrati, M., Goubert, E., Gensac, E., others, 2019. Holocene sediment
1203 mobilization in the inner continental shelf of the Bay of Biscay: Implications for regional
1204 sediment budget offshore to onshore. *Journal of Coastal Research* 88, 110–121.
1205
- 1206 Mielck, F., Holler, P., Bürk, D., Hass, H., 2015. Interannual variability of sorted bedforms in
1207 the coastal German Bight (SE North Sea). *Continental Shelf Research* 111, 31–41.
1208
- 1209 Miselis, J.L., McNinch, J.E., 2006. Calculating shoreline erosion potential using nearshore
1210 stratigraphy and sediment volume: Outer Banks, North Carolina. *Journal of Geophysical*
1211 *Research: Earth Surface* 111.
1212
- 1213 Murray, A.B., Coco, G., Goldstein, E.B., 2014a. Cause and effect in geomorphic systems:
1214 Complex systems perspectives. *Geomorphology* 214, 1–9.
1215
- 1216 Murray, A.B., Goldstein, E.B., Coco, G., 2014b. The shape of patterns to come: from initial
1217 formation to long-term evolution. *Earth Surface Processes and Landforms* 39, 62–70.
1218
- 1219 Murray, A.B., Thieler, E.R., 2004. A new hypothesis and exploratory model for the formation
1220 of large-scale inner-shelf sediment sorting and “rippled scour depressions”. *Continental*
1221 *Shelf Research* 24, 295–315.
1222
- 1223 Naffaa, M., Fanos, A., El Ganainy, A., 1995. Prediction of closure depth at the Nile delta
1224 coast. *Alexandria Engineering Journal* 34, 167–173.
1225
- 1226 Nicholls, R.J., Birkemeier, W.A., Hallermeier, R.J., 1997. Application of the depth of closure
1227 concept, in: *Coastal Engineering 1996*. pp. 3874–3887.
1228

- 1229 Nicholls, R.J., Birkemeier, W.A., Lee, G., 1998. Evaluation of depth of closure using data
1230 from Duck, NC, USA. *Marine Geology* 148, 179–201.
1231
- 1232 Nicholls, R.J., Larson, M., Capobianco, M., Birkemeier, W.A., 1999. Depth of closure:
1233 improving understanding and prediction, in: *Coastal Engineering 1998*. pp. 2888–2901.
1234
- 1235 Niedoroda, A.W., Swift, D.J., 1981. Maintenance of the shoreface by wave orbital currents
1236 and mean flow: observations from the Long Island coast. *Geophysical Research Letters* 8,
1237 337–340.
1238
- 1239 Niedoroda, A.W., Swift, D.J., Hopkins, T.S., Ma, C.-M., 1984. Shoreface morphodynamics
1240 on wave-dominated coasts. *Marine Geology* 60, 331–354.
1241
- 1242 Nnafie, A., de Swart, H., Calvete, D., Garnier, R., 2014. Effects of sea level rise on the
1243 formation and drowning of shoreface-connected sand ridges, a model study. *Continental*
1244 *Shelf Research* 80, 32–48.
1245
- 1246 Nnafie, A., de Swart, H.E., Calvete, D., Garnier, R., 2015. Dynamics of shoreface-connected
1247 and inactive sand ridges on a shelf, Part 2: The role of sea level rise and associated
1248 changes in shelf geometry. *Continental Shelf Research* 104, 63–75.
1249
- 1250 Oakley, B.A., Murphy, C., Varney, M., Hollis, R.J., 2019. Spatial Extent and Volume of the
1251 Shoreface Depositional Platform on the Upper Shoreface of the Glaciated Rhode Island
1252 South Shore. *Estuaries and Coasts* 1–20.
1253
- 1254 Ojeda, E., Ruessink, B., Guillen, J., 2008. Morphodynamic response of a two-barred beach to
1255 a shoreface nourishment. *Coastal Engineering* 55, 1185–1196.
1256
- 1257 Ortiz, A.C., Ashton, A.D., 2016. Exploring shoreface dynamics and a mechanistic
1258 explanation for a morphodynamic depth of closure. *Journal of Geophysical Research:*
1259 *Earth Surface* 121, 442–464.
1260
- 1261 Patterson, D., Nielsen, P., 2016. Depth, bed slope and wave climate dependence of long term
1262 average sand transport across the lower shoreface. *Coastal Engineering* 117, 113–125.
1263
- 1264 Pham, D.T., Gouramanis, C., Switzer, A.D., Rubin, C.M., Jones, B.G., Jankaew, K., Carr,
1265 P.F., 2017. Elemental and mineralogical analysis of marine and coastal sediments from
1266 Phra Thong Island, Thailand: Insights into the provenance of coastal hazard deposits.
1267 *Marine Geology* 385, 274–292.
1268
- 1269 Pilkey, O.H., Young, R.S., Riggs, S.R., Smith, A.S., Wu, H., Pilkey, W.D., 1993. The
1270 concept of shoreface profile of equilibrium: a critical review. *Journal of Coastal Research*
1271 9, 255–278.
1272
- 1273 Plets, R.M., Callard, S.L., Cooper, J.A.G., Kelley, J.T., Belknap, D.F., Edwards, R.J., Long,
1274 A.J., Quinn, R.J., Jackson, D.W., 2019. Late Quaternary sea-level change and evolution of
1275 Belfast Lough, Northern Ireland: new offshore evidence and implications for sea-level
1276 reconstruction. *Journal of Quaternary Science* 34, 285–298.
1277

- 1278 Preston, J., Hurst, M.D., Mudd, S.M., Goodwin, G.C., Newton, A.J., Dugmore, A.J., 2018.
1279 Sediment accumulation in embayments controlled by bathymetric slope and wave energy:
1280 Implications for beach formation and persistence. *Earth Surface Processes and Landforms*
1281 43, 2421–2434.
1282
- 1283 Pretorius, L., Green, A.N., Cooper, J.A., 2018. Submerged beachrock preservation in the
1284 context of wave ravinement. *Geo-Marine Letters* 38, 19–32.
1285
- 1286 Raff, J.L., Shawler, J.L., Ciarletta, D.J., Hein, E.A., Lorenzo-Trueba, J., Hein, C.J., 2018.
1287 Insights into barrier-island stability derived from transgressive/regressive state changes of
1288 Parramore Island, Virginia. *Marine Geology* 403, 1–19.
1289
- 1290 Ribó, M., Goodwin, I.D., O’Brien, P., Mortlock, T., 2020. Shelf sand supply determined by
1291 glacial-age sea-level modes, submerged coastlines and wave climate. *Scientific Reports*
1292 10, 1–10.
1293
- 1294 Richmond, B.M., Buckley, M., Etienne, S., Chagué-Goff, C., Clark, K., Goff, J., Dominey-
1295 Howes, D., Strotz, L., 2011. Deposits, flow characteristics, and landscape change resulting
1296 from the September 2009 South Pacific tsunami in the Samoan islands. *Earth-Science*
1297 *Reviews* 107, 38–51.
1298
- 1299 Riggs, S.R., Cleary, W.J., Snyder, S.W., 1995. Influence of inherited geologic framework on
1300 barrier shoreface morphology and dynamics. *Marine Geology* 126, 213–234.
1301
- 1302 Robertson, W., Zhang, K., Finkl, C.W., Whitman, D., 2008. Hydrodynamic and geologic
1303 influence of event-dependent depth of closure along the South Florida Atlantic Coast.
1304 *Marine Geology* 252, 156–165.
1305
- 1306 Robertson, W.V., Zhang, K., Whitman, D., 2007. Depth of Closure Derived from Airborne
1307 Laser Bathymetry, in: *Coastal Sediments’ 07*. pp. 1877–1885.
1308
- 1309 Roelvink, J., Stive, M., 1991. Sand Transport on the Shoreface of the Holland Coast: The
1310 Dutch Coast: Paper No. 5, in: *Coastal Engineering 1990*. pp. 1909–1921.
1311
- 1312 Rosenberger, K.J., Storlazzi, C.D., Dartnell, P., 2019. Morphodynamics of a field of crescent-
1313 shaped rippled scour depressions: Northern Monterey Bay, CA. *Marine Geology* 407, 44–
1314 59.
1315
- 1316 Różyński, G., Pruszek, Z., Okroj, T., Zeidler, R., 1999. Depth of closure and seabed
1317 variability patterns, in: *Coastal Engineering 1998*. pp. 2926–2939.
1318
- 1319 Ruggiero, P., Kaminsky, G.M., Gelfenbaum, G., Cohn, N., 2016. Morphodynamics of
1320 prograding beaches: A synthesis of seasonal-to century-scale observations of the Columbia
1321 River littoral cell. *Marine Geology* 376, 51–68.
1322
- 1323 Ruggiero, P., Kaminsky, G.M., Gelfenbaum, G., Voigt, B., 2005. Seasonal to interannual
1324 morphodynamics along a high-energy dissipative littoral cell. *Journal of Coastal Research*
1325 21, 553–578.
1326

- 1327 Russell, P.E., 1993. Mechanisms for beach erosion during storms. *Continental Shelf Research*
1328 13, 1243–1265.
1329
- 1330 Sabatier, F., Stive, M.J., Pons, F., 2005. Longshore variation of depth of closure on a micro-
1331 tidal wave-dominated coast, in: *Coastal Engineering 2004: (In 4 Volumes)*. World
1332 Scientific, pp. 2327–2339.
1333
- 1334 Safak, I., List, J.H., Warner, J.C., Schwab, W.C., 2017. Persistent shoreline shape induced
1335 from offshore geologic framework: effects of shoreface connected ridges. *Journal of*
1336 *Geophysical Research: Oceans* 122, 8721–8738.
1337
- 1338 Schupp, C.A., McNinch, J.E., List, J.H., 2006. Nearshore shore-oblique bars, gravel outcrops,
1339 and their correlation to shoreline change. *Marine Geology* 233, 63–79.
1340
- 1341 Schwab, W.C., Baldwin, W.E., Hapke, C.J., Lentz, E.E., Gayes, P.T., Denny, J.F., List, J.H.,
1342 Warner, J.C., 2013. Geologic evidence for onshore sediment transport from the inner
1343 continental shelf: Fire Island, New York. *Journal of Coastal Research* 29, 526–544.
1344
- 1345 Schwab, W.C., Baldwin, W.E., Warner, J.C., List, J.H., Denny, J.F., Liste, M., Safak, I.,
1346 2017. Change in morphology and modern sediment thickness on the inner continental shelf
1347 offshore of Fire Island, New York between 2011 and 2014: Analysis of hurricane impact.
1348 *Marine Geology* 391, 48–64.
1349
- 1350 Schwab, W.C., Thieler, E.R., Allen, J.R., Foster, D.S., Swift, B.A., Denny, J.F., 2000.
1351 Influence of inner-continental shelf geologic framework on the evolution and behavior of
1352 the barrier-island system between Fire Island Inlet and Shinnecock Inlet, Long Island, New
1353 York. *Journal of Coastal Research* 16, 408–422.
1354
- 1355 Schwartz, R.K., 1975. Nature and genesis of some storm washover deposits. *Coastal*
1356 *Engineering Research Center (US)*.
1357
- 1358 Schwarzer, K., Bohling, B., Heinrich, C., 2014. Submarine hard-bottom substrates in the
1359 western Baltic Sea-human impact versus natural development. *Journal of Coastal Research*
1360 70, 145–150.
1361
- 1362 Shand, R.D., Bailey, D.G., Shepherd, M.J., 1999. An inter-site comparison of net offshore bar
1363 migration characteristics and environmental conditions. *Journal of coastal Research* 15,
1364 750–765.
1365
- 1366 Shawler, J.L., Hein, C.J., Canuel, E.A., Kaste, J.M., Fitzsimons, G.G., Georgiou, I.Y.,
1367 Willard, D.A., 2019. Tidal erosion and upstream sediment trapping modulate records of
1368 land-use change in a formerly glaciated New England estuary. *Anthropocene Coasts* 2,
1369 340–361.
1370
- 1371 Short, A., Jackson, D., 2013. Beach morphodynamics, in: *Treatise on Geomorphology*.
1372 Elsevier, pp. 106–129.
1373
- 1374 Siringan, F.P., Anderson, J.B., 1994. Modern shoreface and inner-shelf storm deposits off the
1375 east Texas coast, Gulf of Mexico. *Journal of Sedimentary Research* 64, 99–110.
1376

- 1377 Slooman, A., Simpson, G., Castellort, S., de Boer, P.L., 2018. Geological record of marine
1378 tsunami backwash: The role of the hydraulic jump. *The Depositional Record* 4, 59–77.
1379
- 1380 Stive, M.J.F., De Vriend, H.J., 1995. Modelling shoreface profile evolution. *Marine Geology*
1381 126, 235–248.
1382
- 1383 Storlazzi, C., Field, M., 2000. Sediment distribution and transport along a rocky, embayed
1384 coast: Monterey Peninsula and Carmel Bay, California. *Marine Geology* 170, 289–316.
1385
- 1386 Swift, D.J., Niedoroda, A.W., Vincent, C.E., Hopkins, T.S., 1985. Barrier island evolution,
1387 middle Atlantic shelf, USA Part I: Shoreface dynamics. *Marine Geology* 63, 331–361.
1388
- 1389 Thieler, E.R., Brill, A.L., Cleary, W.J., Hobbs III, C.H., Gammisch, R.A., 1995. Geology of
1390 the Wrightsville Beach, North Carolina shoreface: Implications for the concept of
1391 shoreface profile of equilibrium. *Marine Geology* 126, 271–287.
1392
- 1393 Thieler, E.R., Foster, D.S., Himmelstoss, E.A., Mallinson, D.J., 2014. Geologic framework of
1394 the northern North Carolina, USA inner continental shelf and its influence on coastal
1395 evolution. *Marine Geology* 348, 113–130.
1396
- 1397 Thieler, E.R., Pilkey Jr, O.H., Cleary, W.J., Schwab, W.C., 2001. Modern sedimentation on
1398 the shoreface and inner continental shelf at Wrightsville Beach, North Carolina, USA.
1399 *Journal of Sedimentary Research* 71, 958–970.
1400
- 1401 Thomas, T., Phillips, M., Williams, A., Jenkins, R., 2011. A multi-century record of linked
1402 nearshore and coastal change. *Earth Surface Processes and Landforms* 36, 995–1006.
1403
- 1404 Trowbridge, J., 1995. A mechanism for the formation and maintenance of shore-oblique sand
1405 ridges on storm-dominated shelves. *Journal of Geophysical Research: Oceans* 100, 16071–
1406 16086.
1407
- 1408 Valiente, N.G., Masselink, G., Scott, T., Conley, D., 2017. Depth of closure along an
1409 embayed, macro-tidal and exposed coast: a multi-criteria approach. *Coast. Dyn* 1211–
1410 1222.
1411
- 1412 Valiente, N.G., Masselink, G., Scott, T., Conley, D., McCarroll, R.J., 2019. Role of waves
1413 and tides on depth of closure and potential for headland bypassing. *Marine Geology* 407,
1414 60–75.
1415
- 1416 Valvo, L.M., Murray, A.B., Ashton, A., 2006. How does underlying geology affect coastline
1417 change? An initial modeling investigation. *Journal of Geophysical Research: Earth Surface*
1418 111.
1419
- 1420 Van de Meene, J.W., van Rijn, L.C., 2000a. The shoreface-connected ridges along the central
1421 Dutch coast—part 1: field observations. *Continental Shelf Research* 20, 2295–2323.
1422
- 1423 Van de Meene, J.W., van Rijn, L.C., 2000b. The shoreface-connected ridges along the central
1424 Dutch coast—part 2: morphological modelling. *Continental Shelf Research* 20, 2325–
1425 2345.
1426

- 1427 Van der Molen, J., Van Dijck, B., 2000. The evolution of the Dutch and Belgian coasts and
1428 the role of sand supply from the North Sea. *Global and Planetary Change* 27, 223–244.
1429
- 1430 Verwaest, T., Houthuys, R., Roest, B., Dan, S., Montreuil, A.-L., 2020. A Coastline
1431 Perturbation caused by Natural Feeding from a Shoreface-connected Ridge (Headland
1432 Sint-André, Belgium). *Journal of Coastal Research* 95, 701–705.
1433
- 1434 Vincent, C.E., Young, R.A., Swift, D.J., 1983. Sediment transport on the Long Island
1435 shoreface, North American Atlantic Shelf: role of waves and currents in shoreface
1436 maintenance. *Continental Shelf Research* 2, 163–181.
1437
- 1438 Vis-Star, N.C., De Swart, H., Calvete, D., 2007. Effect of wave-topography interactions on
1439 the formation of sand ridges on the shelf. *Journal of Geophysical Research: Oceans* 112.
1440
- 1441 Wijnberg, K.M., 2002. Environmental controls on decadal morphologic behaviour of the
1442 Holland coast. *Marine Geology* 189, 227–247.
1443
- 1444 Wright, L., Boon, J., Kim, S., List, J., 1991. Modes of cross-shore sediment transport on the
1445 shoreface of the Middle Atlantic Bight. *Marine Geology* 96, 19–51.
1446
- 1447 Wright, L., Short, A., Green, M., 1985. Short-term changes in the morphodynamic states of
1448 beaches and surf zones: an empirical predictive model. *Marine geology* 62, 339–364.
1449
- 1450 Wright, L., Short, A.D., 1984. Morphodynamic variability of surf zones and beaches: a
1451 synthesis. *Marine geology* 56, 93–118.
1452
- 1453 Yoshikawa, S., Nemoto, K., 2014. The role of summer monsoon-typhoons in the formation of
1454 nearshore coarse-grained ripples, depression, and sand-ridge systems along the Shimizu
1455 coast, Suruga Bay facing the Pacific Ocean, Japan. *Marine Geology* 353, 84–98.
1456
- 1457 Zecchin, M., Catuneanu, O., Caffau, M., 2019. Wave-ravinement surfaces: classification and
1458 key characteristics. *Earth-science reviews* 188, 210–239.
1459
1460